Tectono-metamorphic evolution of an evaporitic décollement as recorded by mineral and fluid geochemistry: The "Nappe des Gypses" (Western Alps) case study

Guillaume Barré, Pierre Strzerzynski, Raymond Michels, Stephane Guillot, Pierre Cartigny, Emilie Thomassot, Catherine Lorgeoux, Nelly Assayag, Laurent Truche

Tectono-metamorphic evolution of an evaporitic décollement as recorded by mineral and fluid geochemistry: the "Nappe des Gypses" (Western Alps) case study

Guillaume Barré[1*], Pierre Strzerzynski[2], Raymond Michels[1], Stéphane Guillot[3], Pierre Cartigny[4], Emilie Thomassot[5], Catherine Lorgeoux[1], Nelly Assayag[4], Laurent Truche[3]

[1]*Université de Lorraine, CNRS, GeoRessources, UMR 7359, BP 70239, F-54506 Vandoeuvre-lès-Nancy, France*

[2]*Laboratoire de Géologie UFR Sciences et Technique, CNRS, UMR6112, Université du Mans, Avenue O. Messiaen, 72000 Le Mans, France*

[3]*Univ. Grenoble Alpes, Univ. Savoie Mont Blanc, CNRS, IRD, IFSTTAR, ISTerre, 38000 Grenoble, France*

[4]*Institut de Physique du Globe de Paris (IPGP), 1 Rue Jussieu, 75005 Paris, France*

[5]*CNRS, CRPG, UMR 7359, 15 rue Notre Dame des Pauvres, F-54500 Vandoeuvre-lès-Nancy, France*

[*]*e-mail: guillaume.barre@univ-pau.fr*

Abstract

Evaporites play a major role on the structuration of collisional orogens especially when they act as décollement units. However, their exact pressure-temperature-deformation (P-T-d) paths are poorly documented. In this study, the first direct P-T-d constraints of the "Nappe des Gypses" formation (western French Alps) have been established. An innovative association of structural geology, petrography, crystallochemistry, and detailed study of both fluid inclusions and stable isotopes (C, O) analysis has been applied to this evaporitic facies. Geochemical

analysis shows that the “Nappe des Gypses” formation has recorded the three typical metamorphic and deformational events of the Alps (namely D1, D2 and D3). These different constraints allow the determination of the first determination of the P-T path for this unit. Metamorphic peak conditions of the “Nappe des Gypses” are at 16.6 ± 2.3 kbars and 431°C ± 28°C. This formation was buried at similar conditions than the oceanic units. During the exhumation path, the D1-D2 transition is reached at 350°C ± 20°C and 6.5 ± 1.8 kbars and the D2-D3 transition is assumed to be at 259°C ± 24°C and 2.0 ± 1.0 kbars (Strzerzynski et al., 2012). Peak P-T conditions overlap those of the median Liguro-Piemontese units but are different from those of the Briançonnais units. It implies 1) an active and crucial role of the “Nappe des Gypses” during the exhumation of the Alpine oceanic complex. And 2) confirms the allochthonous and more distal origin of the European Thetysian passive margin of the “Nappe des Gypses” formation. Consideration of sulfates dehydration probably between 15.0 and 16.6 kbars and 200 and 300°C, allows to discuss pore pressure excess and its mechanical consequences on the exhumation process. This process is very likely to amplify the "décollement" effect of the evaporites and allow the nappe stack formation.

This illustrates the role of this formation as a décollement surface. This difference of evolution highlights the major role of the evaporitic formations on the exhumation and structuration of a collisional chain. Such methodology could contribute to decipher the role of evaporites in the structural context of other collisional chains such as Himalaya, Pyrenees or Zagros.

Keywords: Alps, Evaporites, Décollement, Metamorphism, Fluid inclusions, Stable Isotopes analysis

1. Introduction

Evaporites are found all over the world in fold and thrust belts including among others: Alps (e.g., Malavieille and Ritz, 1989; Graham et al., 2012), Himalaya (e.g., Baker et al., 1988), Pyrénées (e.g., Canérot et al., 2005), Turkey (e.g., Kergaravat et al., 2016), Zagros (e.g., Callot et al., 2012). Evaporites are well documented in many orogenic structures as remarkable décollement layers (Davis and Engelder, 1985; Vendeville et al., 2017). Geomechanical experiments and models both under compressive (e.g., Costa and Vendeville, 2002; Gemmer et al., 2005; Dooley et al., 2012) and extensive regimes (e.g., Vendeville et al., 1995) have brought a series of key information on its mechanism. For example, it is shown that excess of pore pressure induced by the dehydration of gypsum into bassanite and anhydrite (e.g., Ko et al., 1997; Leclère et al., 2016), are related to occurrences of earthquakes. However, the overall role of evaporites during subduction followed by exhumation is not fully understood due to the lack of major silicates assemblage in evaporitic units. This study aims at unravelling the motion of such a décollement layer and the processes responsible for the weakening of evaporites in this peculiar context by taking the "Nappe des Gypses" evaporitic formation (Western Alps) as a case study.

In the Alps the "Nappe des Gypses" evaporitic formation is described as a major décollement layer (e.g., Malavieille and Ritz, 1989) between the external and the internal Briançonnais zones and is considered as having played a major role in nappe formation and hence structuration of major tectonic units. The "Nappe des Gypses" formation was specifically studied for its geotechnical properties (Fabre and Dayre, 1982), composition of fluid inclusions (Grappin et al., 1979) and for saline water springs related to the evaporites (Zuppi et al., 2004).

This formation is either studied as an independent unit (e.g., Jaillard, 1985) or integrated as part of the Briançonnais cover (Gabalda et al., 2009), the Vanoise cover (Lanari et al., 2014) or

the Modane-Aussois unit (Strzerzynski et al., 2012). Whatever its tectonic association, this layer always occurs structurally below the Jurassic/Cretaceous Liguro-Piemontese units.

Even if the internal Alps have been widely studied during the late decades, only few results focused on the "Nappe des Gypses". Only one temperature estimates of 420°C has been reported so far for the metamorphic peak (Gabalda et al., 2009) and no pressure estimate is presently available. This lack of data is probably due to the nature of dominant rock lithology (anhydrite and dolomite) which is not optimal for structural, metamorphic or geochronology studies. This study proposes for the first time a multi-technique investigation documenting the petrography, the deformation features, pressure and temperature history of the "Nappe des Gypses" in order to decipher its burial/exhumation evolution within the framework of the western Alps geological history.

2. Geological settings

2.1. General structural context of the studied area

The internal Alps consists of a stack of continental and oceanic-margin derived nappes emplaced and metamorphosed during the Cenozoic (Fig. 1; e.g. de Graciansky et al., 2010). The "Nappe des Gypses" unit corresponds to hundreds of meters (from 100 to 400 m) of dominant massive anhydrite interbedded with dolomites and micaschists layers from centimetric to plurimetric thickness (Fig. 2). The "Nappe des Gypses" formation corresponds to a typical marine basin wide evaporites depositions (Warren, 2010) characterized by large sulfates accumulation during an extension phase of late Triassic (Carnian) as evidenced by the presence of *Equisetum* fossils in schists layers embedded in the evaporites (Fudral et al., 1994). The "Nappe des Gypses" unit is covered by Liguro-Piemontese units. It consists of ophiolitic assemblages derived from Upper Jurassic oceanic crust (metagabbro, metabasalts) and mantle

remnants characterized by serpentinites embedded into Cretaceous metasediments called "Schistes Lustrés" (e.g., Agard et al., 2002; Ganne et al., 2007). The contact between the “Nappe des Gypses” and the Liguro-Piemontese units is of tectonic origin induced by the presence of evaporitic rocks that favored strain localization (e.g., Davis and Engelder, 1985).

The Briançonnais zone corresponds to a continental basement covered by Carboniferous to Eocene deposits (Strzerzynski et al., 2012 and references therein). To the east, lower to middle Triassic detritic deposits, schists and carbonates are the most abundant whereas to the west, carboniferous conglomerates, sandstones, black shales and anthracite form the “Zone Houillère” (e.g., Mercier and Beaudoin, 1987; Barféty et al., 2006; Lanari et al., 2012). The hundred meters thick Liassic carbonates and calcschists of the Dent Parrachée unit forms the syn-rift series announcing the opening of the Liguro-Piemontese oceanic domain (e.g., Platt and Lister, 1985). This unit has been sometime associated with the “Nappe des Gypses” unit (Gabalda et al., 2009).

As the evaporites of the “Nappe des Gypses” unit have sedimented after the early to middle Triassic Briançonnais deposits, it has been often proposed that the “Nappe des Gypses” forms the direct continuation of the Briançonnais units (Mascle et al., 1988). However, the nature of the contact between the “Nappe des Gypses” and the Briançonnais units is still debated.

2.2. Regional tectonic and metamorphic evolution

The internal part of the Western Alps experienced a complex polyphased tectonic evolution that takes place in a general context of subduction/exhumation. Three tectonic phases are distinguished and called thereafter the D1, D2 and D3 events. Even if these events present structural similarities, recent studies have highlighted several changes in the relationships between tectonic events and metamorphic P-T path (e.g., Schwartz et al., 2009; Lanari et al., 2014). In addition, precise datings highlight a younging of successives tectono-metamorphic

events toward the west (Agard et al., 2002; Ganne et al., 2007; Gerber, 2008; Strzerzynski et al., 2012).

1) The D1 event consists of a top-to-the north to north-west thrusting phase characterized by intense deformations, isoclinal folding and formation of the D1 foliation oriented sub-parallel to S0 (Agard et al., 2002; Ganne et al., 2007; Strzerzynski et al., 2012; Lanari et al., 2012). It is responsible of the formation of the internal nappe stack of the Liguro-Piemontese unit over the European margin. Within the Briançonnais units, it is also responsible for the formation of several tectonic slices such as the internal crystalline massifs, the internal and external Briançonnais units (Strzerzynski et al., 2012; Lanari et al., 2012). The D1 event occurred during the metamorphic peak and the early stage of exhumation. P-T conditions are up to 570°C, 22-24 kbar in the Liguro-Piemontese unit (Agard et al., 2001; Plunder et al., 2012), 500°C and 15 kbar in the internal Briançonnais zone (Ganne et al., 2007; Strzerzynski et al., 2012) and 270 - 350°C and 8 to 10 kbar in the external Briançonnais zone (Lanari et al., 2012; Strzerzynski et al., 2012). Time constrains of the D1 event indicate that it occurred first at ca. 66-55 Ma within the oceanic units (Agard et al., 2002), then into the internal crystalline massifs and the internal part of the Briançonnais units between 55 and 43 Ma (Meffan-Main et al., 2004; Ganne et al., 2007; Rosenbaum et al., 2012) and finally into the external Briançonnais units between 45 and 35 Ma (Strzerzynski et al., 2012).

2) The D2 event is characterized by the top-to-the east shear zone associated with large folds. A S2 schistosity developed under greenschist facies and affected the whole D1 nappe stack (Ganne et al., 2007; Lanari et al., 2012; Strzerzynski et al., 2012). The tectonic significance of the D2 event is still debated. In the most internal part of the belt, top-to-the east D2 shear is frequently parallel to the D1 foliation and interpreted as detachment (Agard et al., 2002; Ganne

et al., 2007). In the external Briançonnais units, the top-to-the east event is related to backthrusting and backfolding in a context of thickening of the belt (Lanari et al., 2012). Both extensional D2 detachment and backthrusting occurred at the transition between internal and external Briançonnais units and are very difficult to distinguish (Strzerzynski et al., 2012). Time constrains suggest that extensional top-to-the east shear zone occurred earlier within the oceanic unit (50-40 Ma; Agard et al., 2002), and then migrated into the internal crystalline massif (43-35 Ma; e.g., Ganne et al., 2007). Ages of the backthrusting are comprised between 35 and 32 Ma in the Briançonnais units (e.g., Strzerzynski et al., 2012).

3) The D3 event corresponds to the formation of large dome into the nappe stack in association with faulting (Ganne et al., 2007). It is responsible of the last stage of exhumation below 300°C accompanied by a top-to-the west tilting phase within the Liguro-Piemontese unit (Schwartz et al., 2009) in a context of polyphase brittle tectonics (Champagnac et al., 2006). Deformations occurred during the Miocene and probably are still active today (Delacou et al., 2004).

3. Sampling and analytical methods

3.1. Sampling

The ″Nappe des Gypses″ formation was sampled from 6 major outcrops in the internal part of the western French Alps. They were selected to cover most of the geographical extent along the tectonic contact with the Briançonnais units, near the villages of Modane, Bramans, and Sollières-l'Envers (Arc Valley), the Mont-Cenis lake, the Roubion stream (near Névache village) and Tignes lake (Fig. 1). Lithologies as well as structural features were recognized as to bring geological background to rocks facies and mineral assemblages (e.g. in fractures).

3.2. Petrography

Hand samples as well as thin and thick sections were studied for petrography, mineralogy and fluid inclusions. In addition, X-ray Diffraction (XRD) analyses were performed on micaschists layers sampled on each studied site to determine their mineralogy using a ®Bruker D2 Phaser diffractometer, with Cu-Kα radiation. Diffractograms were interpreted using EVA software and spectra comparison to the NIST database. Micas may not be distinguished from their clay alteration products using solely XRD spectra because of similar chemical and crystallographic properties. To ensure the identification of unaltered micas, elemental compositions of micaschists layers were obtained using a Cameca computer-controlled SX-100 Electron Microprobe (EMP) equipped with a wavelength dispersive spectrometer (WDS). The accelerating voltage was set at 15 kV, beam current at 12 nA and peak counting time varied from 10 to 20s for silicates. The EMP analyses were used to determine pressure in the "Nappe des Gypses*"* formation using the phengite thermobarometer of Dubacq et al. (2010). This technique is based on the K-white micas hydration calculated on the basis of their elemental composition determined by EMP. As the host-rock corresponds to gypsum dehydration into anhydrite (Grappin et al., 1979), we consider that water is available in abundance in the system. Therefore, we fixed the water activity at 1. This allows a simultaneous estimation of the pressure and nH2O at a given temperature. The method of Dubacq et al. (2010) to estimate pressure requires that the temperatures were already determined on chlorite associated with phengite. As no chlorite where found to be associated with the phengite, we used the temperatures previously determined by Raman Spectroscopy of Carbonaceous Material (RSCM), fluid inclusions and stable isotopes.

3.3. Raman Spectroscopy of Carbonaceous Material (RSCM)

The maximum temperature of metamorphism was deduced using the geothermometer of Beyssac et al. (2002). This technique is based on the variation of the organization of

carbonaceous material and the integration of the Raman band area typical of graphite. Raman spectra were recorded on a Labram spectrometer (®Jobin-Yvon, Horiba) using a 514 nm (green) Ar^+ laser excitation with a laser power of 200 mW. A filter was used to reduce the laser power on the sample at around 1 mW to prevent samples degradation during acquisition. Each acquisition was performed using a grating of 1800 lines/mm, a slit width of 100 μm and a confocal hole of 500 μm providing a spectral resolution of 1 to 1.5 cm^{-1}.

3.4. Fluid inclusions analysis

Fluid inclusions were studied on double polished 200 μm-thick sections from samples of i) anhydrite ± quartz ± fluorite veins present in the dolomitic "boudins", ii) automorph albites mineral hosted in some dolomitic "boudins" and iii) quartz veins associated to micaschists layers (see section 4.2. below for petrological description).

Microthermometric measurements were performed on a Linkam THMSG600 heating-cooling stage connected to an Olympus BX51 microscope. The stage was calibrated using synthetic and natural fluid inclusions with the following phase transitions: the ice melting of pure H_2O at 0.0°C and the critical homogenization temperatures (T_h) of natural fluid inclusions at 374.0°C. The accuracy for total homogenization temperatures is about ±1°C, according to the calibration curves. Total homogenization temperatures were measured in inclusions hosted in quartz, albite and fluorite. Due to high deformation of the crystal and change of the internal volume during heating, T_h measurements from fluid inclusions hosted in anhydrite and fluorite are given for indicative purpose and for comparison with T_h obtained in syngenetic quartz-hosted fluid inclusions.

3.5. Carbon and oxygen isotopes analysis of dolomite

Carbon and oxygen isotopic compositions of dolomite were determined by using an auto sampler Gasbench coupled to a Thermo Scientific MAT253 isotope ratio mass spectrometer (IRMS). Each mineral phase was collected as 2 to 1000 mg of powder using a Dremel tool with boreholes of 1 and 2 mm in diameter. This procedure allows better targeting the desired mineral phases of <1 mm diameter whatever the host environment. Samples powder was then reacted with 2 mL of supersaturated orthophosphoric acid at 70°C during 5h in a He atmosphere. 10 measurements cycles of the isotopic composition of produced CO_2 were performed. All samples measurements were adjusted to an internal reference calibrated on the international standards IAEA CO-1, IAEA CO-8 (Stichler, 1995) and an in-house dolomite standard. C and O isotopic measurements were performed at CRPG laboratory (Vandœuvre-Lès-Nancy, France) and systematically doubled in order to check homogeneity of analyses. Isotopic compositions are reported in δ notation (in ‰) relative to V-PDB for carbon and converted to V-SMOW for oxygen. Standard deviations were 0.1‰ and 0.05‰ for $\delta^{18}O$ and $\delta^{13}C$ respectively.

Carbon and oxygen isotope compositions allow to determine the isotopic fractionation ($\Delta^{13}C$ and $\Delta^{18}O$) between two adjacent mineral phases (here gray and white dolomite). It is assumed that the isotopic equilibrium is reached when the two adjacent phases are directly bonded in similar structural positions (e.g., tension gashes). C and O isotope fractionation equations between dolomite and water in one hand (Golyshev et al., 1981; Horita, 2014), and dolomite and dissolved CO_2 in the other hand (Golyshev et al., 1981; Ohmoto and Rye, 1979) were used to determine equilibrium temperature between the two adjacent carbonates. At isotopic equilibrium, this temperature corresponds to the precipitation temperature of the newly precipitated white dolomite (Valley, 2001). Only samples from Névache outcrop do not allow equilibrium

temperature determination due to the lack of associated primary and secondary dolomites samples.

4. Results

4.1. Rock formations and deformations of the "Nappe des Gypses"

The "Nappe des Gypses" unit corresponds to an evaporitic sedimentary unit consisting of evaporites (mainly anhydrites), marine carbonates (dolomite), shales and clay layers (micaschists). Anhydrite rock is the most abundant rock formation of the unit. It forms massive outcrops all along the Arc valley in the Bramans, Sollières, Ambin outcrops and ruiniform landscape marked by numerous sinkholes in the Mont-Cenis lake area. Sedimentary bedding is underlined in white anhydrite by numerous pale gray layers that are commonly folded. Due to massive recrystallization, alpine foliations are most of the time invisible.

Marine carbonates have been observed in all sampling area. They consist of centimeter to meter scale bed of gray dolomite where for instance fine stromatolitic lamines are preserved (Fig. 3A-B). In the Bramans area, marine carbonates beds present automorph to sub-automorph albite (Fig. 3F and Supplementary Fig. A1) that forms crystals with X-Carlsbad and twins called “Roc Tourné” (Rais et al., 2008). As these carbonate beds have been strongly folded and stretched by alpine tectonics, they form various scale blocks more or less rounded and elongated within the main anhydrite layering, called “boudins”. A secondary white dolomite, in which no sedimentary structures are visible, is frequently observed around marine carbonate blocks. White dolomite probably formed by dissolution of a part of the gray dolomite beds and re-crystallization.

Sedimentary clay layers are observed in each studied outcrop and present variable local thickness ranging from the plurimetric (Fig. 2C-D-F) to the microscopic scale (Fig. 4). They

have been transformed into micaschist by alpine metamorphism where white micas are abundant and underline alpine foliations. Shales are scarcer as they have only been observed in Ambin stream and in Roubion stream near Névache village (Supplementary Fig. A2). They contain organic matter that leads to the formation of graphite during the metamorphism which is then used for the RSCM technique.

4.1.1. D1 deformations

At the regional scale, the D1 deformation is related to the nappes emplacement onto the Briançonnais unit (e.g., Ganne et al., 2007; Strzerzynski et al., 2012). On the studied outcrops, such a dominant simple shear deformation induces a very penetrative deformation of anhydrite layers. Marine carbonate beds, micaschists and shales are folded, thinned and stretched. This produce spectacular isoclinal recumbent folds hinges (Fig. 2F), and "boudins" of the gray dolomitic beds (Fig. 2A,G). White dolomite crystals of mm to cm size form pressure shadows located between gray dolomite “boudins”. This leads us to propose that these white dolomites crystallize during the stretching of the dolomite bed during D1 folding (Fig. 2E). Within clays layers, micas crystallize and underline a first foliation thereafter called D1 foliation. As D1 folding is isoclinal, bedding use to be transposed to the D1 foliation (Fig. 2A). This tectonic sequence is recognized in all of the studied outcrops (Fig. 2).

4.1.2. D2 foliation (S2)

Large scale D2 deformations are evidenced by the evolution of the S0-S1 structures from a site to another. For example, between the Sollières and the Ambin stream outcrops (Fig. 1), the main beddings dip to the SW and to the NE forming a syncline structure. From these outcrops, we estimate a N30-N45° striking fold axis postdating D1 structure that is compatible with D2

structures as observed elsewhere (e.g., Ganne et al., 2007; Gerber, 2008; Lanari et al., 2014; Strzerzynski et al., 2012).

At the outcrop scale (Sollières, Névache and Mont-Cenis lake outcrops), D2 folds affect the D1 foliation and a very discrete D2 foliation underline the D2 fold axis planes (Fig. 2D). Within micaschist layers, D2 foliation, when present, is more penetrative and forms a crenulation foliation associated with a second generation of white micas (Fig. 4). At the Mont-Cenis, the main layering of the anhydrite rocks is here sub-horizontal (Fig. 2C). This layering cut some micaschists and dolomite blocks displaying a vertical foliation. Very similar relationships are observed in the Ambin Massif with the association of an early vertical D1 and a late D2 foliation (Ganne et al., 2007). This suggests that D2 deformation is ~~strongly~~ expressed in the Mont Cenis area (Fig. 2C and 4A).

Thin sections from the Bramans outcrop illustrate the relative relationships between white micas and albite: observations reveal that albite crystallize between two white micas crystallization phases (Fig. 4B). We propose, according to the surrounding area (Ganne et al., 2007; Gerber, 2008; Strzerzynski et al., 2012), that albite crystallization, including D1 white micas, is surrounded by D2 white micas and then marks the very beginning of the D2 deformation phase (Fig 4).

4.1.3. D3 tectonics

In all sampling sites, late brittle structures are very scarce and late faults in evaporite rocks have not been clearly identified. In many places, dolomitic beds are affected by an intense fracturation without preferred orientation rather suggesting an episode of hydraulic fracturing postdating the D1 event (Fig. 3E). From available evidences, temporal relationship between this episode and the D2 structure cannot been established. These observations are in agreement with

the global deformation history of the Vanoise cover during the Alpine subduction along the Briançonnais and Liguro-Piemont suture zone (e.g., Lanari et al., 2012).

4.2. Temperatures determination

4.2.1. C and O isotopes signatures and equilibrium temperatures in dolomite

Carbon and oxygen isotope compositions ($\delta^{13}C$ and $\delta^{18}O$ respectively) were determined on 50 dolomite samples collected in all the 6 studied outcrops. We collected micritic gray dolomites of sedimentary (primary) origin and white dolomite that crystallize during alpine events (Fig. 2G). We distinguished during sampling a first white dolomite generation that is associated with D1 structures from a second generation, postdating D1 deformations that is observed all around gray dolomitic beds without preferential orientation (Fig. 2E-H).

Sedimentary "boudins" of gray dolomite present $\delta^{18}O$ values around 23.75‰$_{V\text{-}SMOW}$ ± 1.49 and $\delta^{13}C$ values around 3.50‰$_{PDB}$ ± 0.63. The D1 well-crystallized white dolomite presents $\delta^{18}O$ values around 20.63‰$_{V\text{-}SMOW}$ ± 2.44 and $\delta^{13}C$ values around 2.85‰$_{PDB}$ ± 1.04. In Sollières, Bramans, Ambin and Mont-Cenis outcrops, obtained isotopic equilibrium temperatures for the D1 white dolomites present the same range of temperature between 330°C and 432°C with a mean at 383°C ± 30°C, whereas temperatures at the Tignes outcrop seems to be shifted to higher temperature between 385°C and 475°C with a mean at 436°C ± 46°C (Table 1).

The later white dolomite surrounding the gray dolomitic "boudins" displays $\delta^{18}O$ values around 16.95‰$_{V\text{-}SMOW}$ ± 1.52 and $\delta^{13}C$ values around 1.94‰$_{PDB}$ ± 0.83. All oxygen and carbon stable isotopes values are summarized in Supplementary Table A1. Obtained isotopic equilibrium temperatures on samples from Sollières, Bramans and Ambin stream, ranged between 218°C and 289°C with a mean at 259°C ± 24°C (Table 1).

4.2.2. Fluid inclusions characterization

Our microthermometric data are considered with those from Barré et al. (2017) to bring a general view. Textural observations highlight that mineral phases suitable for fluid inclusions studies are albite, quartz and fluorite. Anhydrite always occurs as micro-crystallized phases indicating continued recrystallization during all the metamorphic events implying scarce and small fluid inclusions. On the contrary, quartz and fluorite appear well crystallized as isolated rounded crystals within the anhydrite (Fig. 3C-D) or within fracture cross cutting gray dolomitic beds. Such an association of quartz and fluorite is observed at Bramans and Sollières outcrops, when only quartz is observed in other studied outcrops. In every case, we never observed quartz and fluorite elongated within the S0-S1 foliation indicating that these minerals postdate the D1 deformation. Albites observed in the Bramans area (Fig. 3F and Supplementary Fig. A1), are of peculiar interest as they probably underline the beginning of the D2 deformation phase as evidenced by their crystallization between D1 and D2 foliation (Ganne et al., 2007; Gerber, 2008; Strzerzynski et al., 2012).

Fluid inclusions are found either isolated or in fracture planes whatever the host mineral (quartz, fluorite or albite). All the fluid inclusions are at least biphasic (aqueous and gaseous phase) and often contain one to three solid phases. All homogenize into the liquid phase, but they present different range of T_h depending on the nature of the host mineral and the sampling sites (Fig. 5; Supplementary Table A2). Considering T_h and fluid inclusions planes intersects in a single grain, it is possible to discriminate different generations (up to 4) of fluid inclusions (Fig. 6). There is a decrease of temperature from the first generation to the last implying episodic recording of the fluid flows during the “Nappe des Gypses” with a cooling from 207°C ± 3°C to 144°C ± 3°C.

Albite records the highest temperatures measured in fluid inclusions with T_h ranging between 330 and 340°C with a mean value at 334°C ± 5°C. In quartz and fluorite, different generations of colder homogenization temperatures are recorded from a site to another: 1) A first generation of fluid inclusions hosted in quartz from Ambin show T_h ranging between 293 and 319°C with a mean at 301°C ± 10°C. 2) A second generation hosted in quartz from the Mont-Cenis lake, show a range of T_h from 230 to 287°C with a mean at 260°C ± 18°C, representing a regional temperature record. 3) A third phase of fluid inclusions trapping is recorded by a second generation of quartz from Ambin and a first generation of fluorite from Sollières l'Envers. The associated T_h range between 203 and 244°C with a mean at 219°C ± 17°C at Ambin, and between 188 and 273°C with a mean at 214°C ± 27°C at Sollières l'Envers. 4) Finally, the last fluid inclusions trapping phase is recorded whatever the hosting mineral (quartz or fluorite) at Bramans, Ambin and Sollières l'Envers outcrops. At Bramans, T_h range between 100 and 185°C with a mean at 137°C ± 28°C. They range between 138 and 179°C with a mean at 153°C ± 15°C at Ambin, and between 98 and 181°C with a mean at 147°C ± 26°C from Sollières outcrops.

The four outcrops studied here present a very similar range of T_h between 50 and 350°C suggesting a very similar thermal evolution. T_h of fluid inclusions hosted by the associated secondary mineral phases (quartz and fluorite) present similar range, confirming the coeval formation of these two minerals.

4.2.3. Graphite geothermometer

Graphite-rich metamorphic shales were collected in Ambin stream and in Roubion stream near Névache village (Supplementary Fig. A2). A total of 51 spectra was recorded from 2 samples from Ambin and 1 sample from Névache (Supplementary Fig. A3). A minimum of 15 spectra per sample was used to determine the temperatures. Table 2 shows the temperature mean

values and the 1σ dispersion obtained from the different spectra per sample. The temperatures were deduced by Raman Spectroscopy of Carbonaceous Material (RSCM) with ranges from 397 to 438°C with a mean at 418°C ± 29°C for Ambin outcrop and at 359°C ± 8°C for Névache outcrop (Table 2).

4.3. Temperature ranges for D1, D2 and D3 event

We interpret the estimated isotopic equilibrium temperature between D1 white and gray sedimentary dolomites as the range of temperature of the D1 event: between 330°C and 432°C in Sollières, Bramans, Ambin and Mont-Cenis outcrops and between 385 and 475°C in the Tignes outcrop (Table 1).

The transition between D1 and D2 deformation phase is constrained in one hand by the lowest D1 isotopic equilibrium temperatures at 356°C ± 21°C (mean of the minimum D1 temperatures per site) and on the other hand by the 334°C ± 5°C T_h on albite from fluid inclusions of the Bramans outcrop. Regarding the proximity and continuity of the outcrops of the Arc Valley (Bramans, Sollières, Ambin) and that of the Mont-Cenis outcrop, we consider similar conditions between these 4 outcrops. This leads us to propose a 350°C ± 20°C temperature for the D1-D2 transition on the Sollières, Bramans, Ambin and Mont-Cenis area.

Temperatures deduced on post-D1 deformation minerals such as quartz and fluorite studied by fluid inclusions analyses and stable isotopes signatures on white dolomites surrounding the dolomitic “boudins”, display temperatures below the D1-D2 transition temperature. This suggests that D2 and later temperatures are never higher than D1 temperature in the "Nappe des Gypses". From a textural and thermal point of view, early fluid inclusions present the higher T_h than the subsequent generations, as expected during a thermal retrograde path.

The maximum temperature of 418°C ± 29°C for Ambin outcrop provided by RSCM is consistent with the maximum 431°C ± 28°C (mean of the maximum D1 temperatures per site) provided by isotopic equilibrium temperature on D1 structure.

Temperature results suggest that maximum metamorphic temperature in the "Nappe des Gypses" is reached during D1 event at 431°C ± 28°C for the Ambin, Sollières, Bramans, Mont-Cenis and Tignes outcrops. Assuming that heating during the early stage of exhumation is never observed in the internal part of western alps, we propose that the maximum temperature is representative of the "Nappe des Gypses" temperature at its maximum of burial. In addition, in absence of heating evidence, we propose that temperatures decrease progressively during exhumation, from 431°C ± 28°C to 356°C ± 21°C during D1 event and then again at lower temperature during events D2 and later, as observed in fluid inclusions (Fig. 6).

4.4. Pressure estimates

White micas are mostly present within micaschist layers of the "Nappe des Gypses". Samples from the Bramans, Ambin stream and Mont-Cenis Lake outcrops contained sufficiently well preserved micaschists layers to allow Electron Microprobe measurement on large enough white micas (Fig. 4). The chemical composition of white micas from these outcrops follows the range of the muscovite–celadonite solid solutions that define phengites (Fig 7B.). Si content of phengite that is related to the crystallization pressure (Massonne and Schreyer, 1989; Vidal et al., 2006; Dubacq et al., 2010) range between 3.54 and 3.27 Si a.p.f.u., 3.44 and 3.16 Si a.p.f.u. and 3.36 and 3.18 Si a.p.f.u. respectively in Bramans, Ambin stream and Mont-Cenis Lake outcrops (Supplementary Table A3 shows typical EMP chemical compositions of phengites used for pressure calculations). As a whole, the wide composition range suggest that a large range of pressure is recorded on the three outcrops. Highest pressures are expected on the Bramans and

Ambin outcrop where phengite are the most Si-rich whereas phengites of the Mont-Cenis Lake outcrop probably only record pressures of D2 deformation according to field observations.

In absence of textural relationships between chlorite and phengite as expected for thermobarometric data (Vidal et al., 2006; Dubacq et al., 2010), continuous estimate of the P-T conditions is not possible on the "Nappe des Gypses". We only provide estimation for the peak condition and the D1-D2 transition considering, in each case, D1 and D2 phengites that give the highest pressures.

According to the field observations and Electron Microprobe measurements, we selected phengites from the Bramans and Ambin outcrops to estimate the maximum conditions at a D1 maximum temperature of 430°C ± 7°C (Table 1) and 418°C ± 29°C, respectively. Obtained pressure range between 15.0 and 18.2 kbar at the Ambin and Bramans outcrops (Fig. 8A-B). We deduce a 5.2 to 7.8 kbars D1-D2 pressure using the highest-pressure results on the Mont-Cenis Lake outcrop at 356°C ± 21°C D1-D2 transition temperature (Fig. 8C). These data allow us to determine a P-T path for the “Nappe des Gypses” formation (Fig. 8D). These values are based on mean temperatures determined from fluid inclusions, Raman spectroscopy and oxygen isotope fractionation calculations. It implies a maximum overestimation of 2 kbars for the low temperature phengites.

5. Discussion

5.1. The maximum P-T condition of the “Nappe des Gypses”.

Our results from the Sollières, Bramans, Ambin stream and Mont-Cenis Lake outcrops are consistent with metamorphic peak conditions with maximum temperature at 431°C ± 28°C and pressure at 16.6 ± 2.3 kbars. Note that the presence of jadeite in the "Nappe des Gypses" formation (e.g., Saliot, 1979; Grappin et al., 1979), is very consistent with these P-T conditions.

The albite-jadeite-quartz line at 431°C is at 11.8 ± 0.5 kbars (Holland, 1980), corresponding to a minimum pressure in the "Nappe des Gypses". From the North-East (Tignes outcrop) to the South-West (Névache outcrop), RSCM temperatures and these obtained on $\Delta^{13}C$ and $\Delta^{18}O$ fractionations in dolomite show that the maximum temperatures increase from 359°C ± 7°C to 475 ± 7°C. As no micaschist layer suitable for pressure estimate was found in the Névache and Tignes outcrops, peak pressure conditions are not constrained. Whatever the pressure, maximum temperatures related to D1 tectonics recorded by the "Nappe des Gypses" increase from the South-West (Névache) to the North-East (Tignes). These temperatures fit perfectly into the North-South and East-West gradients already described in the literature (Beyssac et al., 2002; Gabalda et al., 2009; Lanari et al., 2012; Plunder et al., 2012). Here we highlight for the first time a variation of the P-T conditions during the metamorphic peak within the "Nappe des Gypses".

Metamorphic peak conditions on the Sollières, Bramans, Ambin stream and Mont-Cenis Lake outcrops are in very good agreement (Fig. 9) with maximum conditions reached in the overlying Liguro-Piemontese units (units III and IV after Agard et al., 2002 and Median Units after Plunder et al., 2012). This is also the case with the $\Delta^{13}C$ and $\Delta^{18}O$ fractionation temperatures obtained on the Tignes area as the maximum 475°C is similar with temperatures ranging between 450°C and 475°C in the Liguro-Piemontese units (Median Units after Plunder et al., 2012).

Such a good agreement regarding maximum P-T conditions is not found when comparing the results on the "Nappe des Gypses" and the covered Briançonnais units. In the Ambin Massif and Southern Vanoise unit, even if pressures are the same (14-16 kbars), temperatures are always slightly higher (500°C; Ganne et al., 2007; Gerber, 2008). In the Modane Aussois unit, nor the

pressure (1.1 kbars), nor the temperature (350°C; Gerber, 2008; Strzerzynski et al., 2012) fit with those of the "Nappe des Gypses" and a 5 kbars pressure gap implies very different maximum burial depth. In absence of pressure constraints, comparison with Houiller unit is only based on temperature that decrease from 359°C ± 7°C in the "Nappe des Gypses" to 300°C in the Houiller unit (Lanari et al., 2012).

Assuming these similarities and differences, we propose that the "Nappe des Gypses" recorded HP metamorphism in very similar conditions than the Liguro-Piemontese median units. As Triassic evaporitic formations are older than the Liguro-Piemontese oceanic domain, we propose that the "Nappe des Gypses" has been buried below Liguro-Piemontese units at high pressure conditions during Alpine continental subduction. This implies an initial distal position of evaporitic formations along the European passive margin as observed along current passive margins: Gulf of Mexico (e.g., Jackson and Vendeville, 1994), western Mediterranean Sea (e.g., Lofi et al., 2011) and the Atlantic margins (e.g., Demercian et al., 1993).

Such a burial of the "Nappe des Gypses" may have occurred during the early stage of exhumation of the Liguro-Piemontese units as they reached the same condition than the "Nappe des Gypses". Time constrains suggest a 62-55 Ma to 51-45 Ma range (Agard et al., 2002) for the burial of "Nappe des Gypses" below Liguro-Piemontese units.

The differences between peak conditions of the "Nappe des Gypses" and the Briançonnais units confirm the thrusting of the Triassic evaporitic formations onto the European basements and covers that have recorded various metamorphic conditions. As the nappe stack is folded during D2 event, we proposed that nappe emplacement occurred during the D1 geological event.

5.2. Exhumation of the "Nappe des Gypses"

Exhumation path of the “Nappe des Gypses” occurred in three stages (D1, D2, D3). Our results provide P-T constrains on metamorphic peak (431°C ± 28°C and 16.6 ± 2.3 kbars) and D1-D2 transition (350°C ± 20°C and 6.5 ± 1.8 kbars) conditions. For the D1-D2 transition, as in the case of the metamorphic peak, a good pressure agreement is observed with the Ambin units, whereas temperatures remain higher (500°C; Ganne et al., 2007; Gerber, 2008). This confirms the peculiar thermal evolution of the Ambin massif where a possible heating is described during D2 event (Gerber, 2008). P-T conditions for the D1-D2 transition are consistent with conditions recorded within the Modane-Aussois unit (350°C; Gerber, 2008; Strzerzynski et al., 2012). This confirms our structural observations indicating that the whole nappe stack is folded during D2 event. Such an event has been dated between 43 Ma and 35 Ma (Gerber, 2008; Strzerzynski et al., 2012).

In the surrounding units, D3 phase is characterized by brittle structure (Ganne et al., 2007; Gerber, 2008; Lanari et al., 2014). Fluid inclusions hosted in quartz from carbonate-quartz-sulfide veins provide a maximum 260°C ± 18°C homogenization temperatures (Fig. 5C; Supplementary Table A2) that may represent the D2-D3 transition temperature. This is consistent with the 259°C ± 24°C temperatures obtained on $\Delta^{13}C$ and $\Delta^{18}O$ fractionations on the second type of white-dolomite post-dating the D1 crystallization on the same site (Table 1). Thus, our data are consistent with a temperature of 259°C ± 24°C for the D2-D3 transition. In absence of a more precise structural control on phengite, it is however not possible to deduce a D2-D3 transition pressure based on our own results. Considering this, we propose that D2-D3 transition within the “Nappe des Gypses” and the Modane-Aussois unit are the same at 2.0 ± 1.0 kbars occurred at circa 30 Ma (Gerber, 2008; Strzerzynski et al., 2012).

Our new P-T-d results provide a new highlight on the exhumation of the Liguro-Piemontese units as we demonstrate that its tectonic contact with the “Nappe des Gypses” occurred at pressure as high as 16.6 ± 2.3 kbars. About 10 kbars of exhumation of the Liguro-Piemontese units is related to the D1 phase of the “Nappe des Gypses” in association with NW to W thrusting direction over the Briançonnais unit. At the same time, the internal deformation of the Liguro-Piemontese units is characterized by top to the east direction of shearing in a context of extension (e.g., Tricart, 1984; Agard et al., 2002). These opposite senses of shear that are active during exhumation, are in good agreement with extrusion tectonics model of exhumation (e.g., Godin et al., 2006). Such a scenario implies that the “Nappe des Gypses” unit acted as an efficient "décollement" layer especially as it reaches its metamorphic peak. Figure 10 presents a possible sketch of the kinematic of the western Alps with the integration of the “Nappe des Gypses” tectonic evolution according to our results.

5.3 Phase transitions in the "Nappe des Gypses" and implications for exhumation processes

Evaporite layer such as the “Nappe des Gypses” unit are considered as some of the most efficient "décollement" layers within fold and thrust belts (Davis and Engelder, 1985). Anhydrite which is the most abundant component of the “Nappe des Gypses” unit, forms together with other salts a very soft material regarding to the rheological properties of crustal rocks as it reaches his brittle-ductile transition at around 5 km depth assuming a normal geothermal gradient (Dahlen, 1990). This is consistent with the intense plastic deformation of the “Nappe des Gypses” unit (Fig. 2) and suggests that it can act as an efficient "décollement" layer during the whole burial exhumation path.

Transition phase of gypsum into bassanite and then bassanite into anhydrite release an amount of water estimated at 37% of the initial volume of gypsum (Ko et al., 1997). Recent experimental

investigations on gypsum, bassanite and anhydrite (Yang et al., 2018) better constrain the P-T conditions of these phase transitions (Fig. 9). Dehydration reactions are known to control the slip stabilization of the shearing and to generate pore pressure excess (e.g., Leclère et al., 2016). Gypsum dehydration into bassanite is particularly efficient to generate pore overpressure (Ko et al., 1997). During the prograde path, dehydration reactions may have first transform gypsum into bassanite at ca. 9 kbar and 200°C, then bassanite into anhydrite at ca. 15 kbar and 300°C (Fig. 9; Yang et al., 2018). This suggests that water is released from anhydrite near the end of the exhumation path.

In addition, Grappin et al. (1979) show that the water traps in the “Nappe des Gypses” only come from gypsum dehydration and Triassic connate seawater. Coupled to the pore overpressure generated by gypsum dehydration, it implies that the fluids evolved in a closed system all along the prograde and retrograde paths. Such a fluid overpressure at the metamorphic peak can generate mechanical decoupling and softening effects (Fossen, 2010). We propose that water releases from gypsum to anhydrite transition phases between 9 and 15 kbar and 200 and 300°C, is responsible for the increase of the "décollement" effect of the “Nappe des Gypses” and may have enhanced its exhumation. Such an overpressure event is evidenced, on the field, by hydraulic breccias and hydrothermal veins observed within the dolomite layers (Fig. 3E).

The transition from oceanic subduction to continental subduction between 50 and 40 Ma (HP ophiolites are dated at 45 Ma; Rubatto and Hermann, 2003) most likely marks the implication of the soft “Nappe des Gypses” in the subduction/exhumation dynamics. Consequently, the exhumation of HP units initially controlled by the internal dynamic of the accretionary wedge (Agard et al., 2002; Guillot et al., 2009) evolved to a thrust and fold belt system where the

activation of a décollement layer within Triassic evaporites (Fig. 10) related to dehydration processes and fluid over-pressure play a major role, which was not recognized so far.

6. Conclusions

This study is the first to couple a complete petrographic, geochemical and tectonic investigation from the micro- to the subduction-collision scales of an evaporitic formation. The P-T-d evolution of the “Nappe des Gypses” formation within the Alpine tectonic framework has been determined for the first time. Its main conclusions are:

1. Maximum P-T conditions reached by the “Nappe des Gypses” are 16.6 ± 2.3 kbars and 431°C ± 28°C. These are similar to those reached by the overlying median Liguro-Piemontese units (Plunder et al., 2012) and support 1) an HP tectonic contact between these units and 2) an active role of the “Nappe des Gypses” during the exhumation of the Alpine oceanic complex.
2. Differences in maximum P-T conditions reached by the “Nappe des Gypses” and the Briançonnais units (Ambin, Modane Aussois and Houiller units) confirm allochthonous origin of the "Nappe des Gypses" that is probably originating from a more distal part of the European Tethyan passive margin.
3. Fluid overpressure generated by sulfates dehydration at the end of the prograde path has probably later enhanced exhumation processes at 15.0 to 16.6 kbars.

This integrative study shows how complementary use of petrography, crystallochemistry, fluid inclusions, stable isotopes (C, O) analysis and structural geology allows to constrain the P-T-d path of an evaporitic unit and precise its structural role. This methodology could be applied to other contexts where evaporites play a key role in the geodynamic structuration of orogens (e.g., Pyrénées, Himalaya, Zagros).

Acknowledgements

This work was funded by LABEX ANR-10-LABX-21-01 Ressources21 (Strategic metal resources of the 21st Century) and the French Ministry of Higher Education and Research. The authors are extremely grateful to T. Rigaudier for the C and O stable isotope analysis performed at Centre de Recherches Pétrographique et Géochimiques (CRPG) of Nancy, and to Christophe Scheffer for the pressure estimations calculations. The paper benefited greatly from the review provided by A. Plunder and one anonymous reviewer. We thank P. Agard for his very relevant comments that have improved this paper and for his editorial support.

Appendix A. Supplementary material

Supplementary material related to this article can be found as attached file.

References

Agard, P., Jolivet, L., Goffe, B., 2001. Tectonometamorphic evolution of the Schistes Lustres Complex; implications for the exhumation of HP and UHP rocks in the Western Alps. Bulletin de la Société géologique de France, 172(5), 617-636.

Agard, P., Monié, P., Jolivet, L., Goffé, B., 2002. Exhumation of the Schistes Lustrés complex: in situ laser probe 40Ar/39Ar constraints and implications for the Western Alps. Journal of Metamorphic Geology 20(6), 599-618.

Angiboust, S., Langdon, R., Agard, P., Waters, D., Chopin, C., 2011. Eclogitization of the Monviso ophiolite (W. Alps) and implications on subduction dynamics. Journal of Metamorphic Geology, 30(1), 37-61.

Baker, D.M., Lillie, R.J., Yeats, R.S., Johnson, G.D., Yousuf, M., Zamin, A. S.H., 1988. Development of the Himalayan frontal thrust zone: Salt Range, Pakistan. Geology, 16(1), 3-7.

Barféty, J.C., Polino, R., Mercier, D., Caby, R., Fourneaux, J.C. 2006. Notice explicative de la feuille Névache-Bardonecchia-Modane à 1/50,000. BRGM Feuille, Orléans, p. 160 (in French).

Barré, G., Truche, L., Bazarkina, E.F., Michels, R., Dubessy, J., 2017. First evidence of the trisulfur radical ion S_3^- and other sulfur polymers in natural fluid inclusions. Chemical Geology 462, 1-14.

Beyssac, O., Goffé, B., Chopin, C., Rouzaud, J.N., 2002. Raman spectra of carbonaceous material in metasediments: a new geothermometer. Journal of Metamorphic Geology 20(9), 859-871.

Callot, J. P., Trocmé, V., Letouzey, J., Albouy, E., Jahani, S., Sherkati, S., 2012. Pre-existing salt structures and the folding of the Zagros Mountains. Geological Society, London, Special Publications 363(1), 545-561.

Canérot, J., Hudec, M.R., Rockenbauch, K., 2005. Mesozoic diapirism in the Pyrenean orogen: Salt tectonics on a transform plate boundary. AAPG bulletin 89(2), 211-229.

Champagnac, J.D., Sue, C., Delacou, B., Tricart, P., Allanic, C., Burkhard, M., 2006. Miocene lateral extrusion in the inner western Alps revealed by dynamic fault analysis. Tectonics 25(3), 26 p.

Costa, E., Vendeville, B. C., 2002. Experimental insights on the geometry and kinematics of fold-and-thrust belts above weak, viscous evaporitic décollement. Journal of Structural Geology 24(11), 1729-1739.

Dahlen, F.A., 1990. Critical taper model of fold-and-thrust belts and accretionary wedges. Annual Review of Earth and Planetary Sciences, 18(1), 55-99.

Davis, D.M., Engelder, T., 1985. The role of salt in fold-and-thrust belts. Tectonophysics, 119(1-4), 67-88.

Debelmas, J., 1980. Carte géologique de la France, feuille d'Annecy. B.R.G.M., scale 1/250 000.

Delacou, B., Sue, C., Champagnac, J.D., Burkhard, M., 2004. Present-day geodynamics in the bend of the western and central Alps as constrained by earthquake analysis. Geophysical Journal International 158(2), 753-774.

Demercian, S., Szatmari, P., Cobbold, P.R., 1993. Style and pattern of salt diapirs due to thin-skinned gravitational gliding, Campos and Santos basins, offshore Brazil. Tectonophysics, 228(3-4), 393-433.

Dooley, T.P., Hudec, M.R., Jackson, M.P., 2012. The structure and evolution of sutures in allochthonous salt. AAPG Bulletin 96(6), 1045-1070.

Dubacq, B., Vidal, O., De Andrade, V., 2010. Dehydration of dioctahedral aluminous phyllosilicates: thermodynamic modelling and implications for thermobarometric estimates. Contribution to Mineralogy and Petrology 159(2), 159-174.

Fabre, D., Dayre, M., 1982. Proprietes geotechniques de gypses et anhydrites du trias des alpes de savoie (France). Bulletin de l'Association Internationale de Géologie de l'Ingénieur 25(1), 91-98.

Fossen, H., 2010. Structural Geology. Cambridge University Press (463 pp.).

Fudral, S., Deville, E., Nicoud, G., Pognante, U., Guillot, P., Jaillard, E. (1994). Notice explicative de la feuille Lanslebourg-Mont d'Ambin à 1: 50.000.

Gabalda, S., Beyssac, O., Jolivet, L., Agard, P., Chopin, C., 2009. Thermal structure of a fossil subduction wedge in the Western Alps. Terra Nova 21, 28-34.

Gabudianu Radulescu, I.G., Rubatto, D., Gregory, C., Compagnoni, R., 2009. The age of HP metamorphism in the Gran Paradiso Massif, Western Alps: a petrological and geochronological study of “silvery micaschists”. Lithos, 110(1-4), 95-108.

Ganne, J., Bertrand, J.M., Fudral, S., Marquer, D., Vidal, O., 2007. Structural and metamorphic evolution of the Ambin massif (western Alps): toward a new alternative exhumation model for the Brianconnais domain. Bulletin de la Société Géologique de France 178(6), 437-458.

Gemmer, L., Beaumont, C., Ings, S.J., 2005. Dynamic modelling of passive margin salt tectonics: effects of water loading, sediment properties and sedimentation patterns. Basin Research 17(3), 383-402.

Gerber, W., 2008. Evolution tectono-métamorphique du Briançonnais interne (Alpes Occidentales, massifs de Vanoise Sud et d'Ambin): comportement du socle et de sa couverture dans un contexte de subduction continentale profonde (Doctoral dissertation).

Godin, L., Grujic, D., Law, R.D., Searle, M.P., 2006. Channel flow, ductile extrusion and exhumation in continental collision zones: an introduction. Geological Society, London, Special Publications 268(1), 1-23.

Golyshev, S.I., Padalko, N.L., Pechenkin, S.A., 1981. Fractionation of stable oxygen and carbon isotopes in carbonate systems. Geochemistry International 18, p. 85-99.

de Graciansky, P.C., Roberts, D.G., Tricart, P., 2010. The Western Alps, from rift to passive margin to orogenic belt: an integrated geoscience overview. Elsevier, 429p.

Graham, R., Jackson, M., Pilcher, R., Kilsdonk, B., 2012. Allochthonous salt in the sub-Alpine fold–thrust belt of Haute Provence, France. Geological Society, London, Special Publications 363(1), 595-615.

Grappin, C., Saliot, P., Sabouraud, C., Touray, J. C., 1979. Les variations des rapports Cl/Br, Na/Br et K/Br dans les inclusions fluides des quartz de la cicatrice évaporitique de Bramans-Termignon (Vanoise, Alpes françaises). Chemical Geology 25(1-2), 41-52.

Guillot, S., Hattori, K., Agard, P., Schwartz, S., Vidal, O., 2009. Exhumation processes in oceanic and continental subduction contexts: a review. In Subduction zone geodynamics (pp. 175-205). Springer, Berlin, Heidelberg.

Holland, T.J., 1980. The reaction albite= jadeite+ quartz determined experimentally in the range 600–1200 C. American Mineralogist, 65(1-2), 129-134.

Horita, J., 2014. Oxygen and carbon isotope fractionation in the system dolomite–water–CO_2 to elevated temperatures. Geochimica et Cosmochimica Acta 129, 111-124.

Jackson, M.P.A., Vendeville, B.C., 1994. Regional extension as a geologic trigger for diapirism. Geological society of America bulletin, 106(1), 57-73.

Jaillard, E., 1985. Evolutions sédimentaire et paléotectonique de la zone briançonnaise de Vanoise occidentale (Alpes occidentales françaises). Géologie Alpine 61, 85-113.

Kergaravat, C., Ribes, C., Legeay, E., Callot, J.P., Kavak, K.S., Ringenbach, J.C., 2016. Minibasins and salt canopy in foreland fold-and-thrust belts: The central Sivas Basin, Turkey. Tectonics 35(6), 1342-1366.

Ko, S.C., Olgaard, D.L., Wong, T.F., 1997. Generation and maintenance of pore pressure excess in a dehydrating system 1. Experimental and microstructural observations. Journal of Geophysical Research: Solid Earth 102(B1), 825-839.

Lanari, P., Guillot, S., Schwartz, S., Vidal, O., Tricart, P., Riel, N., Beyssac, O., 2012. Diachronous evolution of the alpine continental subduction wedge: evidence from P–T

estimates in the Briançonnais Zone houillère (France – Western Alps). Journal of Geodynamics 56-57, 39–54.

Lanari, P., Rolland, Y., Schwartz, S., Vidal, O., Guillot, S., Tricart, P., Dumont, T., 2014. P–T–t estimation of deformation in low-grade quartz-feldspar-bearing rocks using thermodynamic modelling and 40Ar/39Ar dating techniques: example of the Plan-de-Phasy shear zone unit (Briançonnais Zone, Western Alps). Terra Nova 26(2), 130-138.

Leclère, H., Faulkner, D., Wheeler, J., Mariani, E., 2016. Permeability control on transient slip weakening during gypsum dehydration: Implications for earthquakes in subduction zones. Earth and Planetary Science Letters 442, 1-12.

Lofi, J., Déverchère, J., Gaullier, V., Gillet, H., Gorini, C., Guennoc, P., Loncke, L., Maillard, A., Sage, F., Thinon, I., 2011. Seismic atlas of the Messinian Salinity Crisis markers in the Mediterranean and Black Seas (Vol. 179, pp. 1-72). Société Géologique de France.

Malavieille, J.T., Ritz, J.F., 1989. Mylonitic deformation of evaporites in décollements: examples from the Southern Alps, France. Journal of Structural Geology 11(5), 583-590.

Mascle, G., Arnaud, H., Dardeau, G., Debelmas, J., Delpech, P.-Y., Dubois, P., Gidon, M., Graciansky, P.-C., Kerckhove, C., Lemoine, M., 1988. Salt tectonics, Tethyan rifting and Alpine folding in the French Alps. Bulletin de la Société géologique de France 4(5), 747-758.

Massonne, H.J., Schreyer, W., 1989. Stability field of the high-pressure assemblage, talc+ phengite and two new phengite barometers. European Journal of Mineralogy, 1(3), 391-410.

Maunder, B., van Hunen, J., Bouilhol, P., Magni, V., 2019. Modeling Slab Temperature: A Reevaluation of the Thermal Parameter. Geochemistry, Geophysics, Geosystems, 20(2), 673-687.

Meffan-Main, S., Cliff, R.A., Barnicoat, A.C., Lombardo, B., Compagnoni, R., 2004. A Tertiary age for Alpine high-pressure metamorphism in the Gran Paradiso massif, Western Alps: A Rb–Sr microsampling study. Journal of Metamorphic Geology 22(4), 267-281.

Mercier, D., Beaudoin, B., 1987. Révision du carbonifère briançonnais: Stratigraphie et évolution du bassin. Géologie Alpine, Mém. H. S. 13, 25–31 (in French).

Ohmoto, H., Rye, R. O., 1979. Isotopes of sulfur and carbon. Barnes HL (ed.) Geochemistry of hydrothermal deposits, 2nd edn. J.

Platt, J.P., Lister, G.S., 1985. Structural history of high-pressure metamorphic rocks in the southern Vanoise massif, French Alps, and their relation to Alpine tectonic events. Journal of Structural Geology 7, 19-35.

Plunder, A., Agard, P., Dubacq, B., Chopin, C., Bellanger, M., 2012. How continuous and precise is the record of P-T paths? Insights from combined thermobarometry and thermodynamic modelling into subduction dynamics (Schistes Lustrés, W. Alps). Journal of Metamorphic Geology 30, 323–346.

Rais, P., Louis-Schmid, B., Bernasconi, S.M., Reusser, E., Weissert, H., 2008. Distribution of authigenic albites in a limestone succession of the Helvetic Domain, eastern Switzerland. Swiss. Journal Geosciences 101(1), 99-106.

Rosenbaum, G., Menegon, L., Glodny, J., Vasconcelos, P., Ring, U., Massironi, M., Thiede, D., Nasipuri, P., 2012. Dating deformation in the Gran Paradiso Massif (NW Italian Alps): Implications for the exhumation of high-pressure rocks in a collisional belt. Lithos, 144, 130-144.

Rubatto, D., Hermann, J., 2003. Zircon formation during fluid circulation in eclogites (Monviso, Western Alps): implications for Zr and Hf budget in subduction zones. Geochimica et Cosmochimica Acta, 67(12), 2173-2187.

Saliot, P., 1979. La jadéite dans les Alpes françaises. Bulletin de Minéralogie, 102(4), 391-401. (in French).

Schwartz, S., Tricart, P., Lardeaux, J.M., Guillot, S., Vidal, O., 2009. Late tectonic and metamorphic evolution of the Piedmont accretionary wedge (Queyras Schistes lustrés, western Alps): Evidences for tilting during Alpine collision. Bulletin of the Geological Society of America 121(3- 4), 502-518.

Stichler, W., 1995. Interlaboratory comparison of new materials for carbon and oxygen isotope ratio measurements. Reference and intercomparison materials for stable isotopes of light elements, 67-74.

Strzerzynski, P., Guillot, S., Leloup, P.H., Arnaud, N., Vidal, O., Ledru, P., Courrioux, G., Darmendrail, X., 2012. Tectono-metamorphic evolution of the Briançonnais zone (Modane-Aussois and Southern Vanoise units, Lyon Turin transect, Western Alps). Journal of Geodynamics 56-57, 55-75.

Tricart, P., (1984). From passive margin to continental collision; a tectonic scenario for the Western Alps. American Journal of Science 284(2), 97-120.

Valley, J.W., 2001. Stable isotope thermometry at high temperatures. Reviews in mineralogy and geochemistry 43, 365–413.

Vendeville, B.C., Ge, H., Jackson, M.P.A., 1995. Scale models of salt tectonics during basement-involved extension. Petroleum Geoscience 1(2), 179-183.

Vendeville, B.C., Pengcheng, T., Graveleau, F., Shaoying, H., Wang, X., 2017. How the presence of a salt décollement in the sedimentary cover influences the behavior of subsalt thrusts in fold-and-thrust belts. Bulletin de la Société géologique de France 188(6), 37.

Vidal, O., De Andrade, V., Lewin, E., Munoz, M., Parra, T., Pascarelli, S., 2006. P–T-deformation-Fe^{3+}/Fe^{2+} mapping at the thin section scale and comparison with XANES mapping: application to a garnet-bearing metapelite from the Sambagawa metamorphic belt (Japan). Journal of Metamorphic Geology, 24(7), 669-683.

Warren, J.K., 2010. Evaporites through time: Tectonic, climatic and eustatic controls in marine and nonmarine deposits. Earth-Science Reviews 98(3), 217-268.

Yang, L., Dai, L., Li, H., Hu, H., Zhuang, Y., Liu, K., Pu, C., Hong, M., 2018 Pressure-induced structural phase transition and dehydration for gypsum investigated by Raman spectroscopy and electrical conductivity. Chemical Physics Letters 706, 151-157.

Zuppi, G.M., Novel, J.P., Dray, M., Darmendrail, X., Fudral, S., Jusserand, C., Nicoud, G., 2004. Eaux fortement minéralisées et circulations profondes dans le socle. Exemple des Alpes franco-italiennes. Comptes Rendus Geoscience 336(15), 1371-1378.

TABLE CAPTIONS

Table 1. Equilibrium temperatures determined from dolomite-H_2O fractionation equations from Golyshev et al. (1981) and Horita (2014) of carbon and oxygen isotopes values.

Table 2. Maximum temperatures obtained by the geothermometer described by Beyssac et al. (2002) on carbonaceous material from black shales layers incorporated in the "Nappe des Gypses" formation.

FIGURE CAPTIONS

Fig. 1. (A) Simplified geological map of the studied area (Western French Alps; modified from Debelmas, 1980) with the corresponding sampling outcrops locations: Né. = Névache – tG. = Bramans – Amb. = Ambin stream – So. = Sollières l'Envers – MC. = Mont-Cenis Lake – Ti. = Tignes. (B) Synthetic cross-section of the studied area in an East-West direction. Maximum temperatures obtained from the different used geothermometer are represented for each studied site.

Fig. 2. Photographs of typical structures observed in the "Nappe des Gypses" formation at the outcrop scale. (A) Typical anhydrite facies with the gray dolomitic "boudins" observed at Bramans outcrops. (B) Anhydrite facies presenting S0/S1 and S2 structures from the Bramans outcrops. (C) Micaschists and anhydrite presenting S0/S1 structures and transposed S2 structures at the Mont-Cenis Lake. (D) Anhydrite recording S0/S1 structures associated to S2 folded micaschists. (E) Gray dolomite recrystallized as white dolomite recording S0/S1 structures, followed to D1 foliation at Sollières l'Envers outcrops. (F) Gray dolomite recorded S0/S1 structures associated to S2 fold marked in micashists layer at Sollières l'Envers outcrops. (G) Representatives D1 tension gashes marked by white dolomite precipitation and following S0/S1

structure, as observed in Sollières l'Envers outcrops. (H) D1 foliation marked in gray-dolomite and associated to S0/S1 structure at Sollières l'Envers outcrops.

Fig. 3. Photographs of typical paragenesis observed in the "Nappe des Gypses" formation. (A and B) Typical stromatolitic dolomite structures as observed in some dolomite "boudins". (C and D) Classically observed quartz and fluorite minerals incorporated in the anhydrite facies. (E) White dolomite and elemental sulfur vein in gray dolomite "boudins". (F) Albites crystals in gray dolomite "boudins". Anh = anhydrite; Qz = quartz; S = native sulfur; Fl = fluorite; G-Dol = gray dolomite; W-Dol = white dolomite; Ab = albite.

Fig. 4. Microphotographs of thin sections at crossed polarized light showing typical microstructures observed in the micaschists and dolomite "boudins". (A) Only D2 structures are marked by micaschists layers in thin section from the Mont-Cenis Lake. (B-C) D1 and D2 structures are recorded by micaschist layers in Bramans thin sections. Albites post-dated D1 structures constrained their crystallization at the D1-D2 transition. D1 veins relics are also still present, together with late D3 veins. Anh = Anhydrite; Dol = dolomite; Qtz = quartz; W-Mca = white micas; Py = Pyrite; Ab = albite.

Fig. 5. Histograms of homogenization temperatures (T_h) obtained by microthermometry on quartz, fluorite, albite and anhydrite-hosted fluid inclusions from Sollières l'Envers, Bramans, Mont-Cenis Lake and Ambin stream outcrops. Detailed data are shown in supplementary Table A2.

Fig. 6. A. Microphotograph of typical fluid inclusions planes hosted in fluorite from Sollières l'Envers outcrop. Mean temperatures associated to each plane are reported together with a sketch representing the relative chronology of the four generations of fluid circulations. It should be noted that the sketch is on a slightly larger scale than that of the photo for the sake of clarity of

the latter. B, C, D and E correspond to microphotographs of a zoom of each plane represented in A.

Fig. 7. (A) Si vs Interlayer cation diagram for analyzed phengites. (B) K-white mica chemistry reported in muscovite, celadonite, pyrophyllite ternary diagram. All compositional data are in per formula unit (p.f.u.) with structural formula calculated on the basis of 11 oxygens.

Fig. 8. (A), (B) and (C) represent the pressure determination for the Bramans, Ambin and Mont-Cenis outcrops, respectively, based on the crossing of the phengites equilibrium curves and the temperature ranges determined by the different geothermometers used in this study. (D) Construction of the P-T path of the "Nappe des Gypses" unit exhumation from the temperatures and pressures data determined in this study. The choice of transitions between events D1, D2 and D3 is explained in section 4.3. in the main text.

Fig. 9. Comparison between "Nappe des Gypses" unit retrograde P-T path and these from the different Briançonnais (in green) and oceanic units (in blue). "Nappe des Gypses" unit estimated prograde P-T path is also represented. They are all plotted in gypsum-bassanite-anhydrite phase diagram from Yang et al. (2018) to determine the maximum conditions of gypsum dehydration. The albite = jadeite + quartz line is also represented (Holland, 1980), with ab = albite; jd = jadeite; qtz = quartz. HZ = Houiller zone (Lanari et al., 2012); MA = Modane-Aussois unit (Strzerzynski et al., 2012); LPU = Liguro-Piemontese Upper unit (Agard et al., 2002); LPM = Liguro-Piemontese Median unit (Plunder et al., 2012); LPL = Liguro-Piemontese Lower unit (Plunder et al., 2012); SV = South-Vanoise unit (Strzerzynski et al., 2012); GP = Gran Paradiso massif (Gabudianu Radulescu et al., 2009); MV = Monviso massif (Angiboust et al., 2011).

Fig. 10. Possible kinematic reconstruction of the Western Alps with highlights on the “Nappe des Gypses” unit from late Eocene to early Miocene. Projection of the surrounding units is also shown at the collision stage. Star represents the location of the “Nappe des Gypses” unit during the tectonic evolution. ZH = Houiller zone; MA = Modane-Aussois unit; SV = South-Vanoise unit; GP = Gran Paradiso massif.

Figure 1

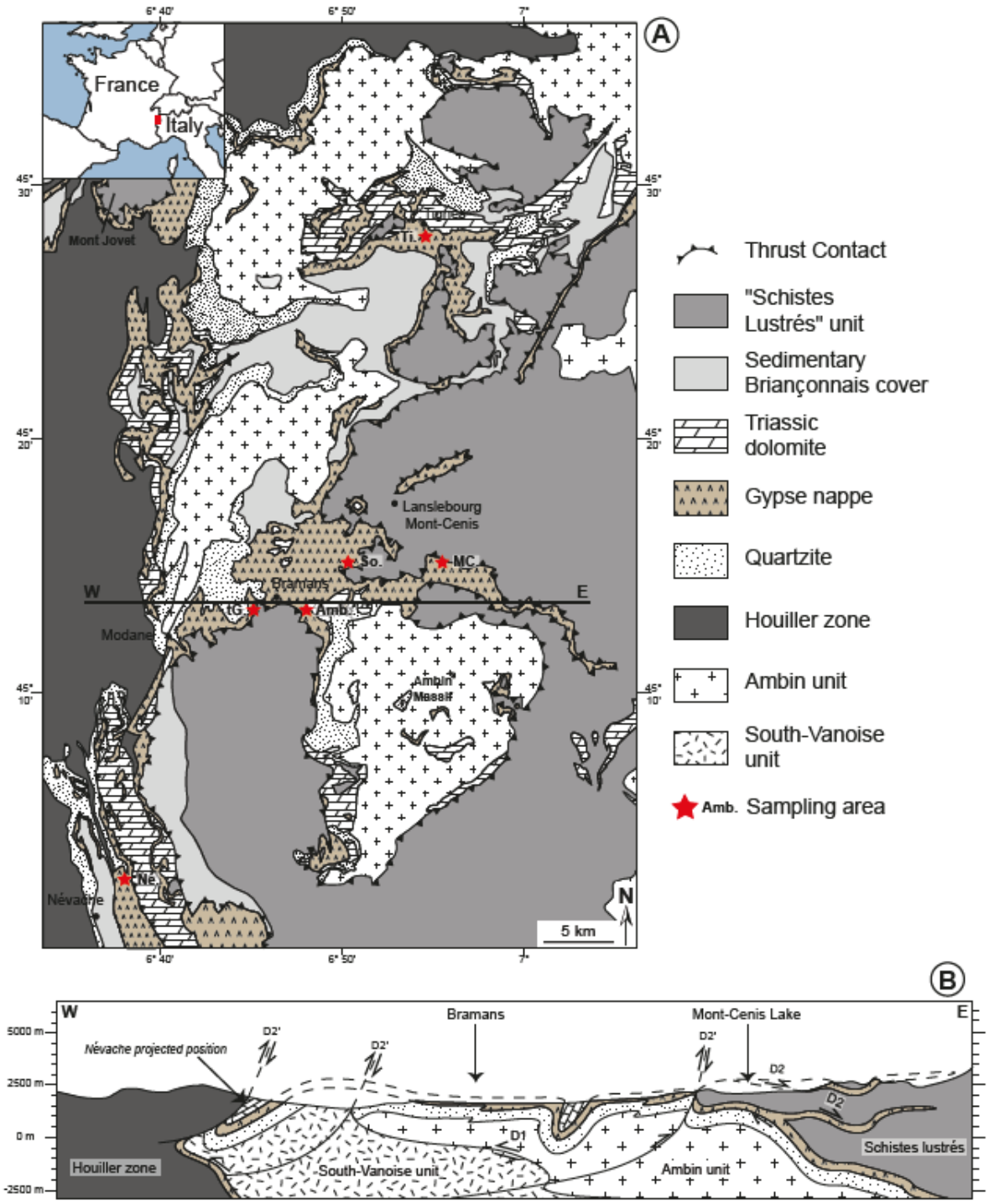
A
France
Italy
6° 40'
6° 50'
7°
45° 30'
45° 20'
45° 10'
Mont Jovet
Lanslebourg
Mont-Cenis
So.
MC
Bramans
W
E
TG
Amb.
Modane
Ambin
Massif
Névache
Ne.
N
5 km
Thrust Contact
"Schistes Lustrés" unit
Sedimentary Briançonnais cover
Triassic dolomite
Gypse nappe
Quartzite
Houiller zone
Ambin unit
South-Vanoise unit
Amb. Sampling area
B
W
E
Bramans
Mont-Cenis Lake
Névache projected position
D2'
D2
D1
5000 m
2500 m
0 m
-2500 m
Houiller zone
South-Vanoise unit
Ambin unit
Schistes lustrés

Figure 2

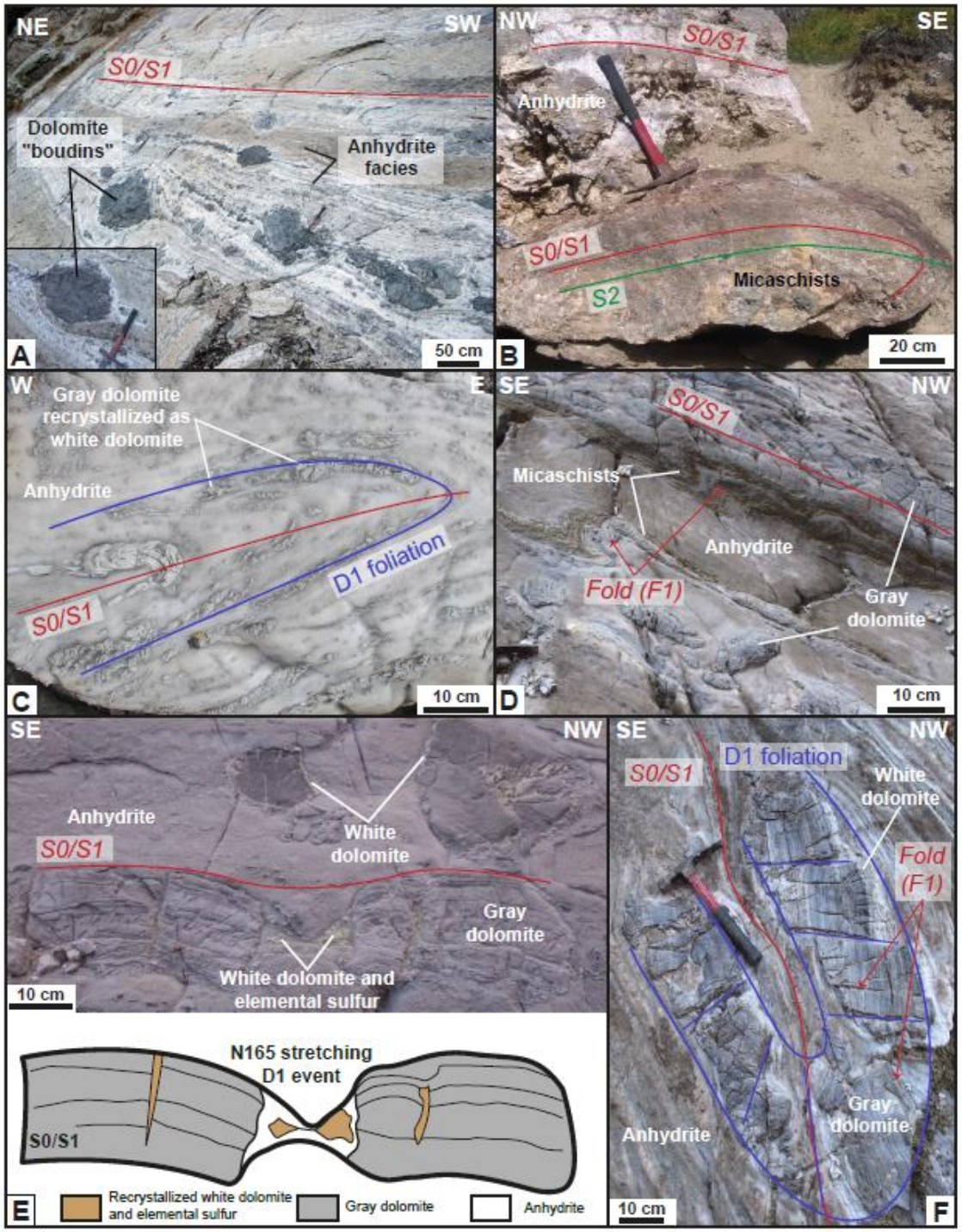
NE
SW
S0/S1
Dolomite "boudins"
Anhydrite facies
A
50 cm
NW
SE
S0/S1
Anhydrite
S0/S1
S2
Micaschists
B
20 cm
W
E
Gray dolomite recrystallized as white dolomite
Anhydrite
D1 foliation
S0/S1
C
10 cm
SE
NW
S0/S1
Micaschists
Anhydrite
Fold (F1)
Gray dolomite
D
10 cm
SE
NW
Anhydrite
S0/S1
White dolomite
Gray dolomite
White dolomite and elemental sulfur
10 cm
SE
NW
S0/S1
D1 foliation
White dolomite
Fold (F1)
Gray dolomite
Anhydrite
10 cm
F
N165 stretching D1 event
S0/S1
E
Recrystallized white dolomite and elemental sulfur
Gray dolomite
Anhydrite

Figure 3

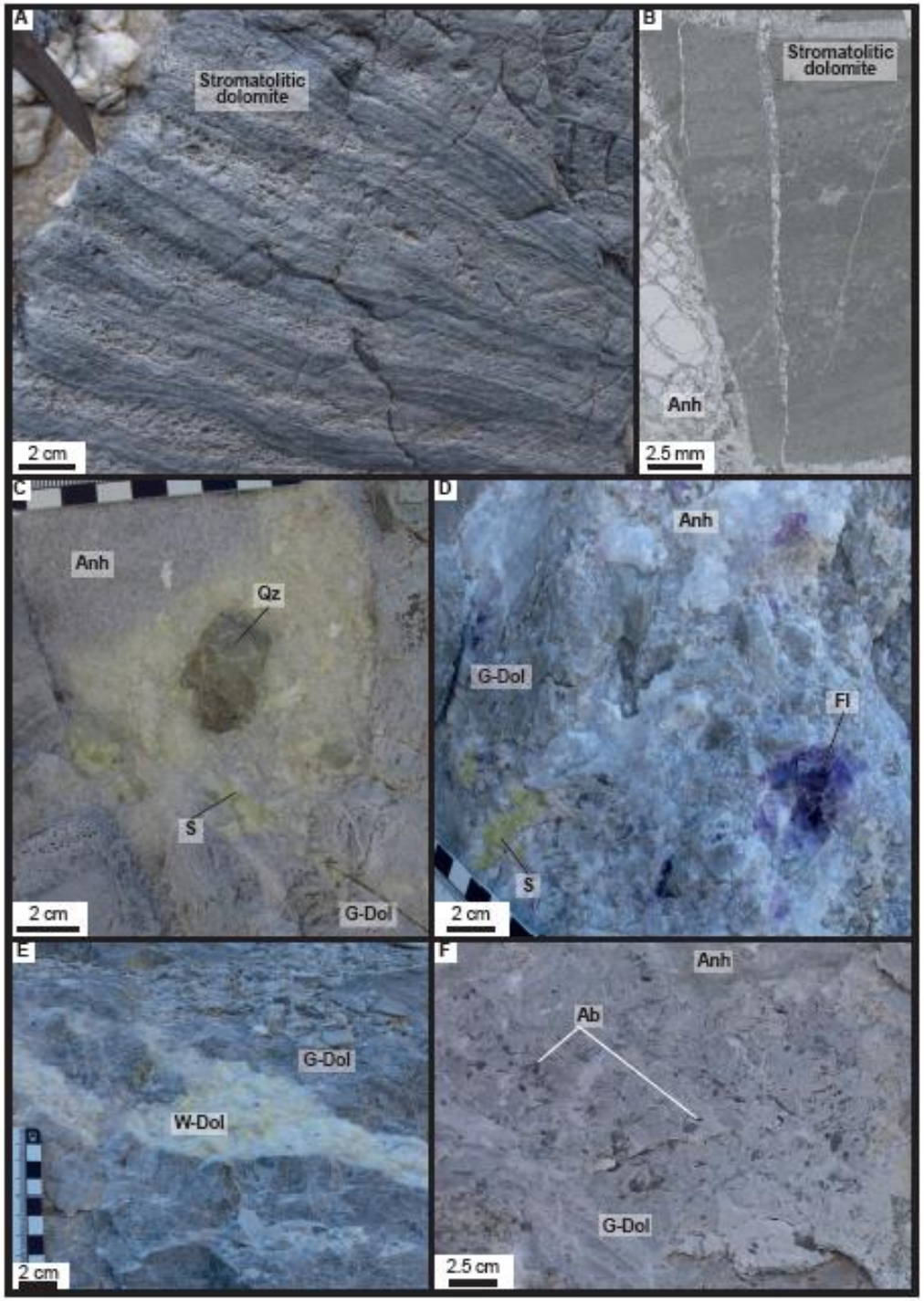
A
Stromatolitic dolomite
2 cm
B
Stromatolitic dolomite
Anh
2.5 mm
C
Anh
Qz
S
G-Dol
2 cm
D
Anh
G-Dol
Fl
S
2 cm
E
G-Dol
W-Dol
2 cm
F
Anh
Ab
G-Dol
2.5 cm

Figure 4

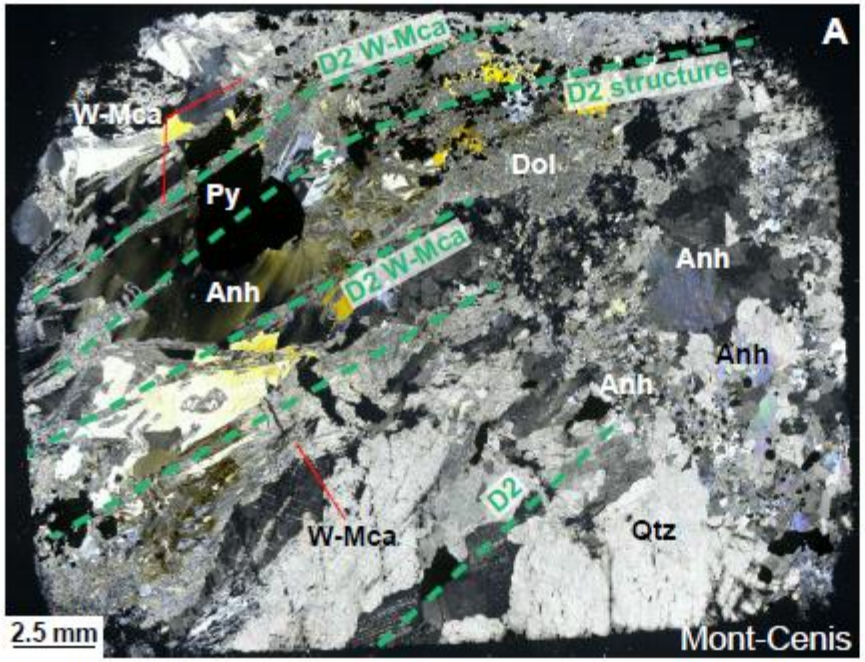

Host-rock

Anh	: anhydrite
Dol	: dolomite

Secondary minerals

W-Mca	: white mica
Qtz	: quartz
Py	: pyrite
Ab	: albite
Fl	: fluorite

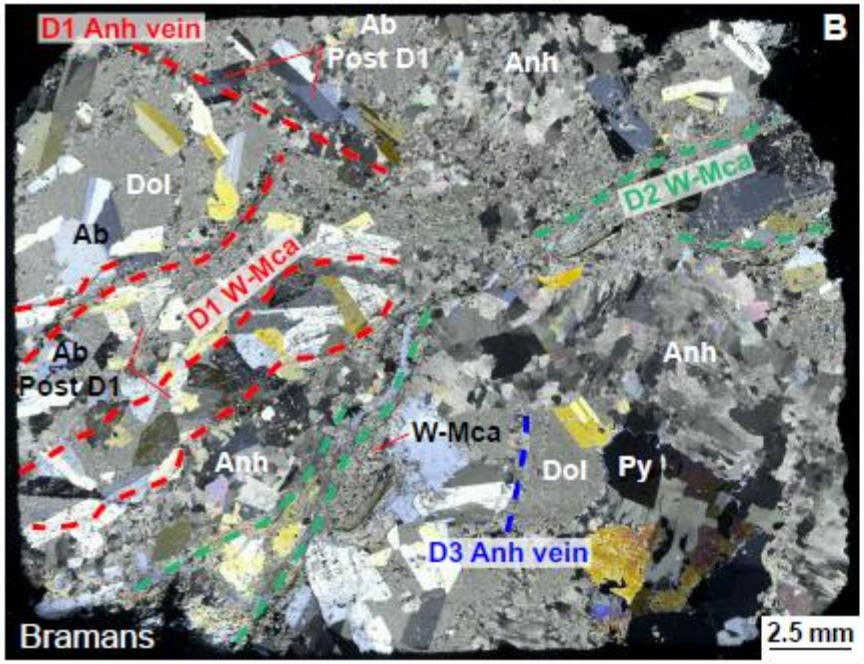

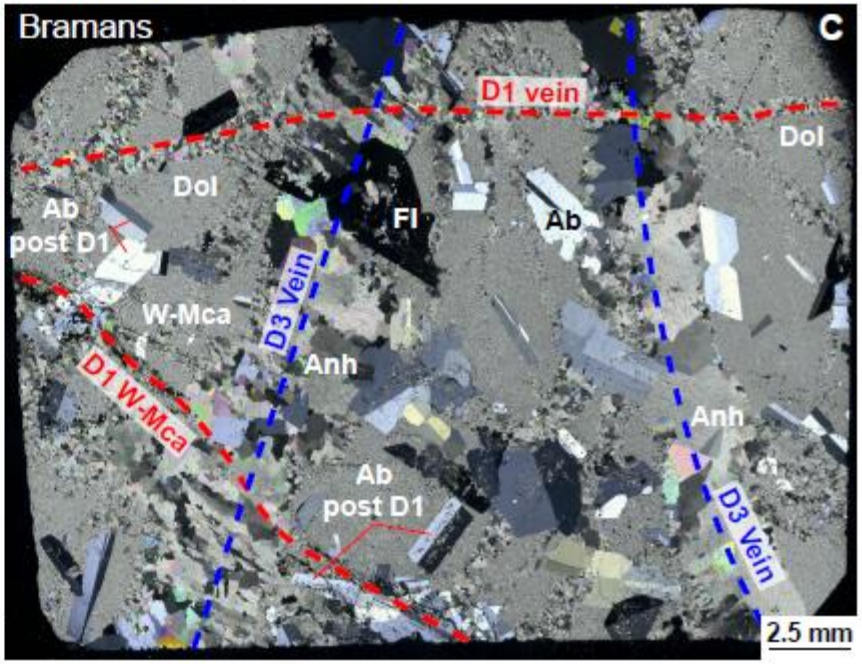

Figure 5

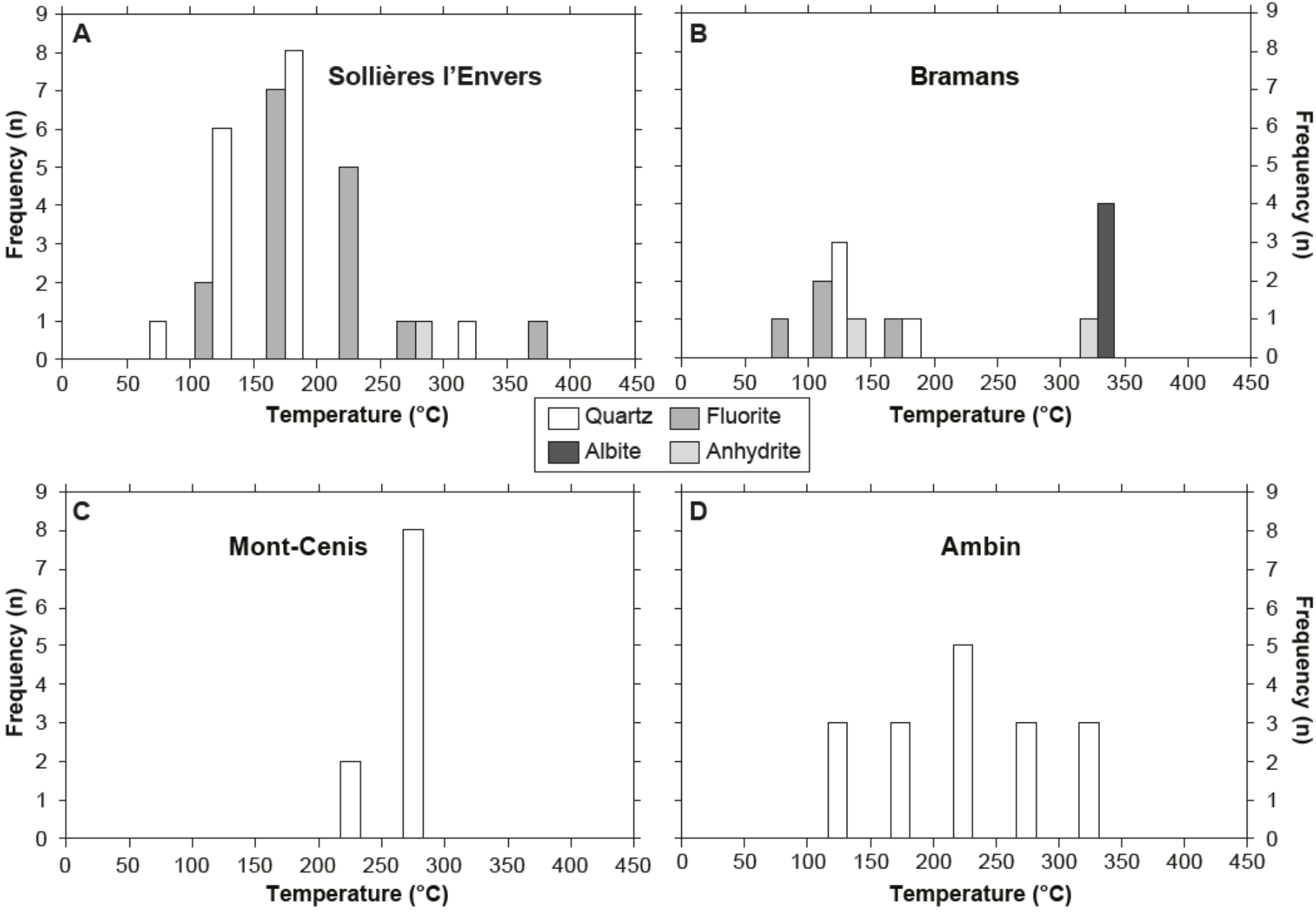
A
Sollières l'Envers
B
Bramans
C
Mont-Cenis
D
Ambin
Frequency (n)
Temperature (°C)
Quartz
Fluorite
Albite
Anhydrite

Figure 6

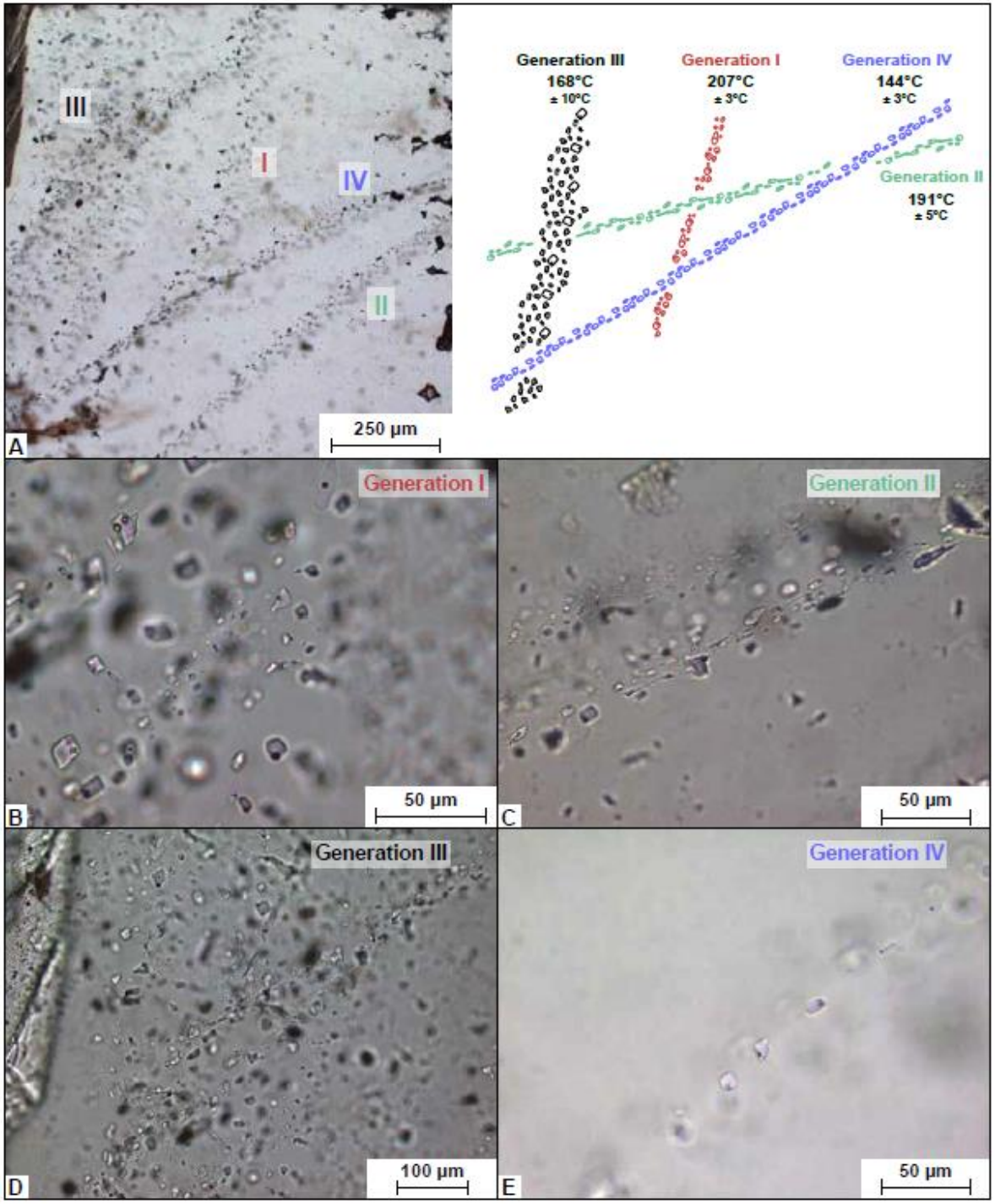
III
I
IV
II
250 µm
A
Generation III
168°C
± 10°C
Generation I
207°C
± 3°C
Generation IV
144°C
± 3°C
Generation II
191°C
± 5°C
Generation I
50 µm
B
Generation II
50 µm
C
Generation III
100 µm
D
Generation IV
50 µm
E

Figure 7

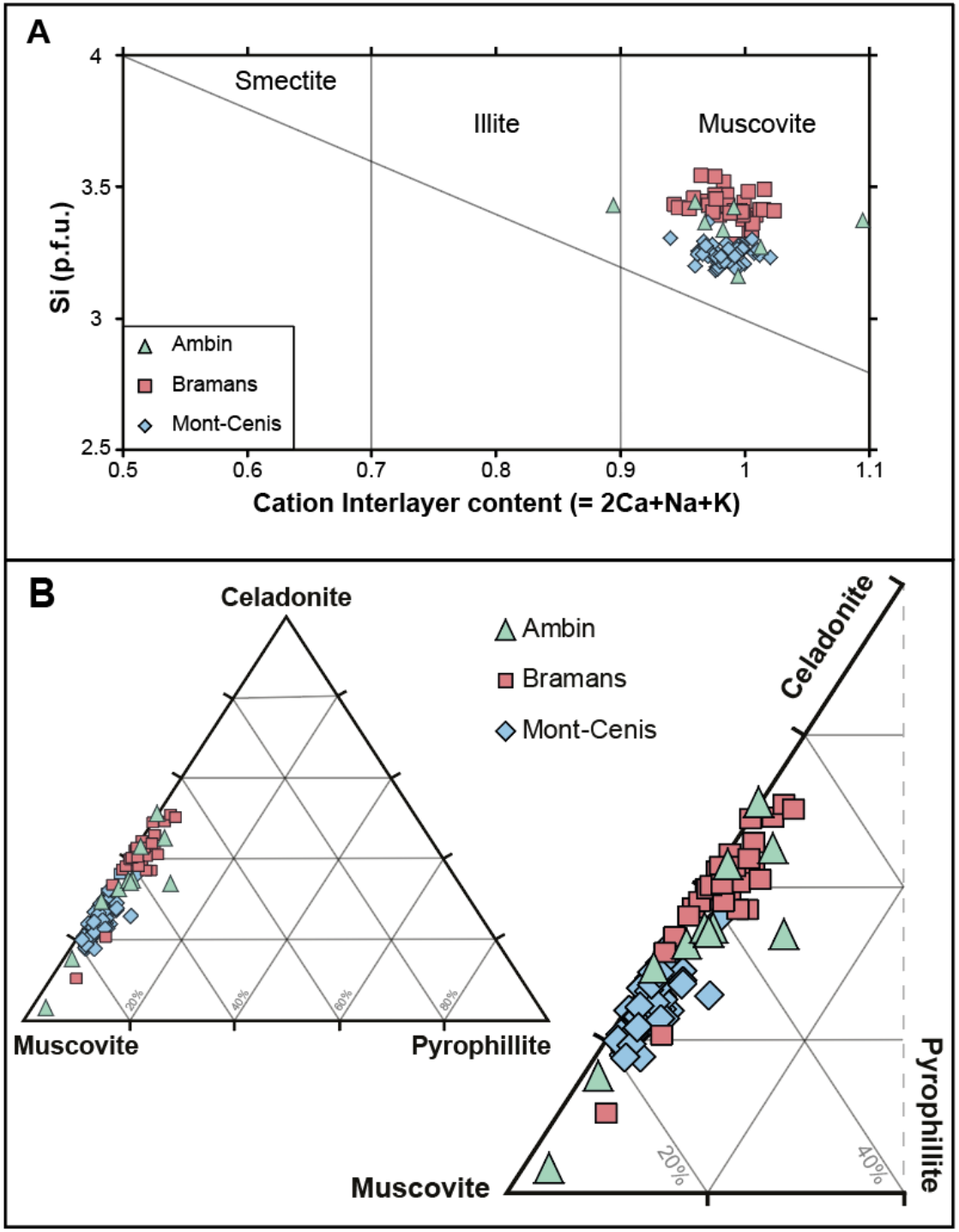
A
Smectite
Illite
Muscovite
Si (p.f.u.)
4
3.5
3
2.5
0.5
0.6
0.7
0.8
0.9
1
1.1
Cation Interlayer content (= 2Ca+Na+K)
Ambin
Bramans
Mont-Cenis
B
Celadonite
Muscovite
Pyrophillite
20%
40%
60%
80%
Ambin
Bramans
Mont-Cenis
Celadonite
Pyrophillite
Muscovite
20%
40%

Figure 8

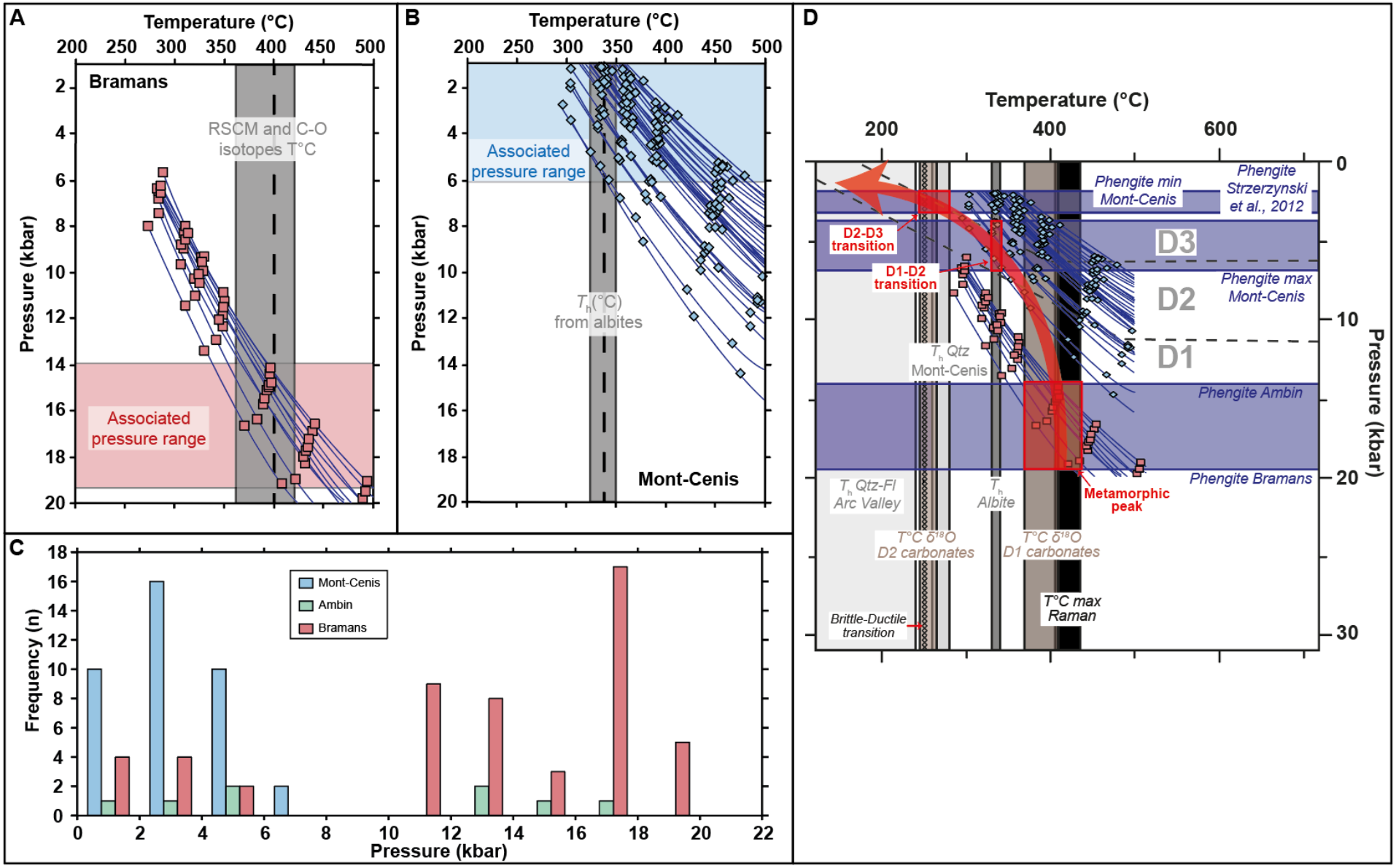
A
Temperature (°C)
200 250 300 350 400 450 500
Bramans
RSCM and C-O isotopes T°C
Associated pressure range
Pressure (kbar)
2 4 6 8 10 12 14 16 18 20
B
Temperature (°C)
200 250 300 350 400 450 500
Associated pressure range
Th(°C) from albites
Mont-Cenis
Pressure (kbar)
2 4 6 8 10 12 14 16 18 20
C
Mont-Cenis
Ambin
Bramans
Frequency (n)
0 2 4 6 8 10 12 14 16 18
0 2 4 6 8 10 12 14 16 18 20 22
Pressure (kbar)
D
Temperature (°C)
200 400 600
Phengite min Mont-Cenis
Phengite Strzerzynski et al., 2012
D2-D3 transition
D3
D1-D2 transition
Phengite max Mont-Cenis
D2
D1
Th Qtz Mont-Cenis
Phengite Ambin
Phengite Bramans
Th Qtz-Fl Arc Valley
Th Albite
Metamorphic peak
T°C δ18O D2 carbonates
T°C δ18O D1 carbonates
T°C max Raman
Brittle-Ductile transition
Pressure (kbar)
0 10 20 30

Figure 9

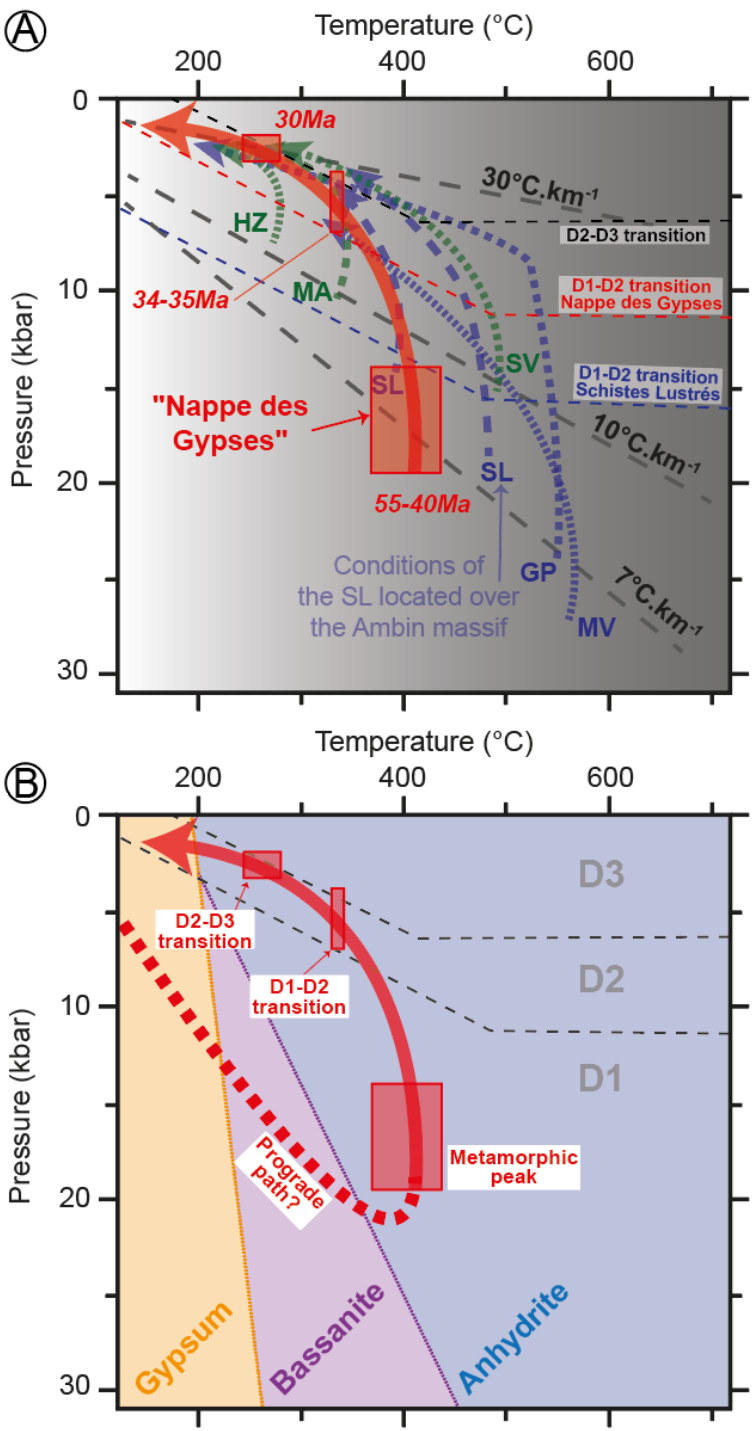
Ⓐ
Temperature (°C)
200
400
600
0
10
20
30
Pressure (kbar)
30Ma
34-35Ma
HZ
MA
SV
SL
"Nappe des Gypses"
55-40Ma
SL
GP
MV
Conditions of the SL located over the Ambin massif
30°C.km-1
D2-D3 transition
D1-D2 transition Nappe des Gypses
D1-D2 transition Schistes Lustrés
10°C.km-1
7°C.km-1
Ⓑ
Temperature (°C)
200
400
600
0
10
20
30
Pressure (kbar)
D3
D2
D1
D2-D3 transition
D1-D2 transition
Prograde path?
Metamorphic peak
Gypsum
Bassanite
Anhydrite

Figure 10

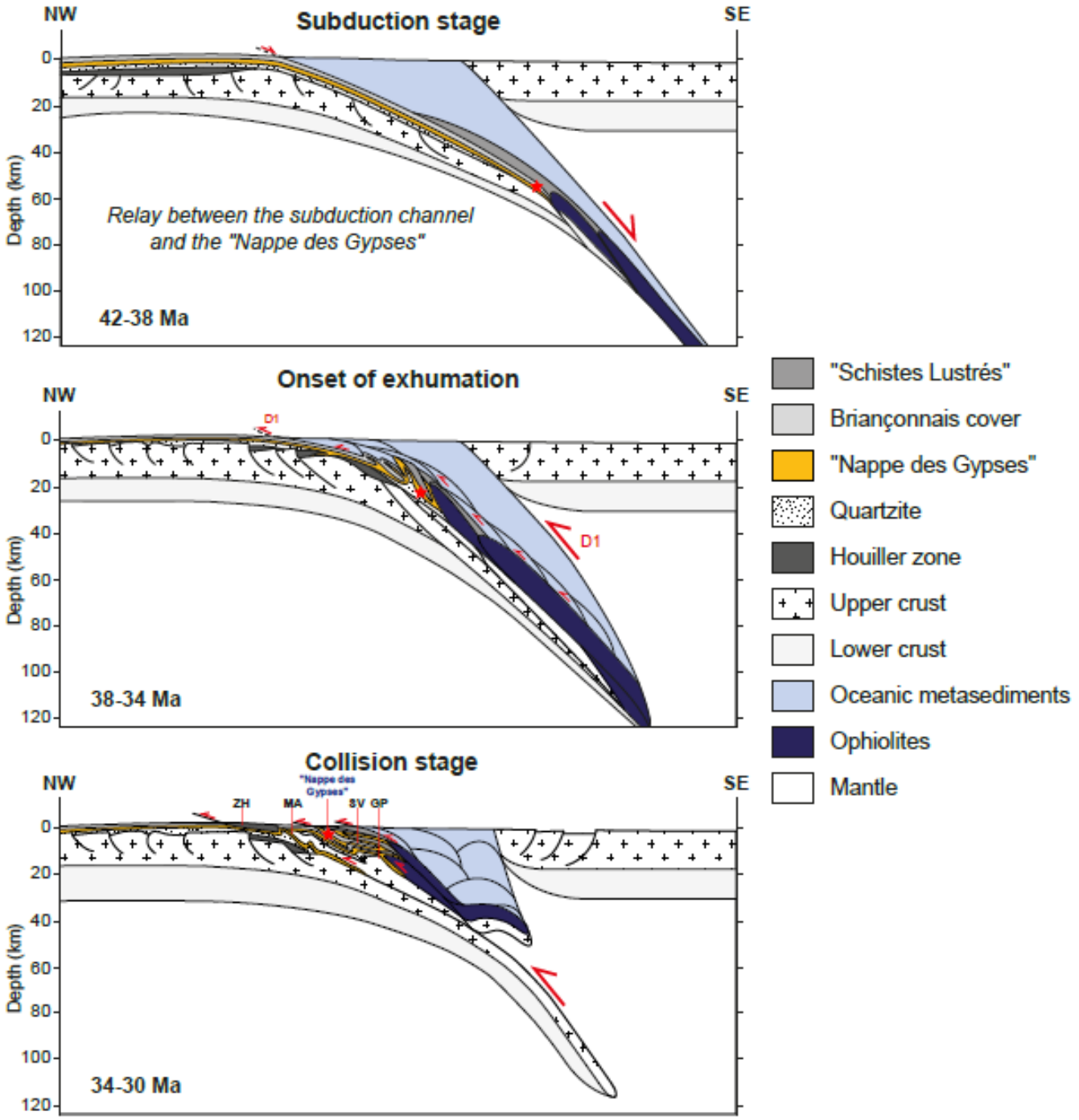
Subduction stage
NW
SE
Depth (km)
0
20
40
60
80
100
120
Relay between the subduction channel
and the "Nappe des Gypses"
42-38 Ma
Onset of exhumation
D1
D1
38-34 Ma
Collision stage
"Nappe des Gypses"
ZH
MA
SV
GP
34-30 Ma
"Schistes Lustrés"
Briançonnais cover
"Nappe des Gypses"
Quartzite
Houiller zone
Upper crust
Lower crust
Oceanic metasediments
Ophiolites
Mantle